ANA BEATRIZ DOS SANTOS

REMOTE SENSING-BASED WATER RESOURCE DIAGNOSIS IN REGIONS WITH INTENSIVE EXPANSION OF IRRIGATION IN BRAZIL

Thesis submitted to the Applied Meteorology Graduate Program of the Universidade Federal de Viçosa in partial fulfillment of the requirements for the degree of *Doctor Scientiae*.

Adviser: Marcos Heil Costa

Co-adviser: Everardo Chartuni Mantovani

VIÇOSA - MINAS GERAIS
2024

Ficha catalográfica elaborada pela Biblioteca Central da Universidade Federal de Viçosa - Campus Viçosa

T
S237r
2024

Santos, Ana Beatriz dos, 1990-
Remote sensing-based water resource diagnosis in regions with intensive expansion of irrigation in Brazil / Ana Beatriz dos Santos. – Viçosa, MG, 2024.
1 tese eletrônica (78 f.): il. (algumas color.).

Texto em inglês.
Orientador: Marcos Heil Costa.
Tese (doutorado) - Universidade Federal de Viçosa, Departamento de Engenharia Agrícola, 2024.
Referências bibliográficas: f. 71-78.
DOI: https://doi.org/10.47328/ufvbbt.2024.090
Modo de acesso: World Wide Web.

1. Irrigação por pivô central. 2. Irrigação agrícola. 3. Sensoriamento remoto. 4. Desenvolvimento de recursos hídricos. I. Costa, Marcos Heil, 1965-. II. Universidade Federal de Viçosa. Departamento de Engenharia Agrícola. Programa de Pós-Graduação em Meteorologia Aplicada. III. Título.

CDD 22. ed. 631.587

Bibliotecário(a) responsável: Bruna Silva CRB-6/2552

ANA BEATRIZ DOS SANTOS

REMOTE SENSING-BASED DIAGNOSIS OF WATER RESOURCES IN REGIONS WITH INTENSIVE EXPANSION OF IRRIGATION IN BRAZIL

Thesis submitted to the Applied Meteorology Graduate Program of the Universidade Federal de Viçosa in partial fulfillment of the requirements for the degree of *Doctor Scientiae*.

APPROVED: February 20, 2024

Assent:

Ana Beatriz dos Santos
Author

Marcos Heil Costa
Adviser

To my parents Cris and Reinaldo.

ACKNOWLEDGEMENTS

To all my family, many thanks for helping and supporting me through life.

To my advisor, Professor Marcos Heil Costa. Your guidance made me who I am today. Working with you for almost twelve years taught me a lot, and I'll always look up to you as I take my own steps forward.

To my co-advisor, Everardo Mantovani, thank you for all the teaching and support. I appreciate you welcoming me as your student and always being there.

To my friends Luiz, Livinha, Flavia, Veronica, Ana, Lucas, Mateus, and Pousa, thanks for the special support during the last months of my doctorate. I appreciate your efforts to make me happy, especially during the challenging times when it was difficult for me.

To all my old friends from the Biosfera-Atmosfera research group, thank you for being like a second family during lonely times. I appreciate having you with me, even though we are physically apart now.

To all my friends from Nebraska, especially Christopher Neale, thank you for warmly welcoming me and teaching me more about evapotranspiration and remote sensing. A special thanks to Regiane, Melli, Thais and Aya for being so supportive and giving me the best hugs and advice, and a big thank to Ivo for all his help – from teaching me how to cross a street in the USA to explaining how a center pivot works.

To Graça Freitas, thanks for all the assistance and support throughout this academic journey.

This study was financed in part by the Coordenação de Aperfeiçoamento de Pessoal de Nível Superior – Brasil (CAPES) – Finance Code 001

To the Conselho Nacional de Desenvolvimento Científico e Tecnológico (CNPq), for granting the scholarship.

ABSTRACT

SANTOS, Ana Beatriz dos, D.Sc., Universidade Federal de Viçosa, February, 2024. **Remote sensing-based water resource diagnosis in regions with intensive expansion of irrigation in Brazil**. Adviser: Marcos Heil Costa. Co-advisers: Everardo Chartuni Mantovani.

Center pivot irrigation has been leading irrigation growth in Brazil in recent years. However, the intensification of climate change effects may lead to issues in regions highly occupied by center pivots. The reduction in precipitation volume or the duration of the dry season often generates conflicts over water usage between irrigators and other water users. Therefore, formulating a diagnosis of the hydrological situation in these regions is crucial. This study selected three Brazilian regions with intensive irrigation expansion: the Corrente and Grande rivers' basins in Bahia and the Alto Rio das Mortes in Mato Grosso. Although these are considered areas with a high technological level in the field, there is no systematic measurement network for water usage yet. Remote sensing products enable the estimation of center pivot water demand through evapotranspiration (ET). For the Corrente and Grande River basins, the MODIS ET product (MOD16A2 Version 6 Evapotranspiration/Latent Heat Flux product) was applied to identify sub-basins with a higher risk of water conflicts. After comparing the estimated irrigation water demand with river flow data, three sub-basins demonstrated a potentially critical situation regarding water resource usage. An in-depth analysis of these sub-basins also revealed that water use by center pivots has steadily increased over the years, pushing water consumption to its limits. In addition to the MODIS product, another database was applied to estimate the irrigation by center pivots, the daily evapotranspiration dataset provided by the GLODET (Global Daily evapotranspiration) platform for the Alto Rio das Mortes. Moreover, ET data measured via eddy covariance were used to assess the accuracy of the two products. The results showed that the new ET dataset exhibited improvements compared to the previous version used, which underestimates evapotranspiration in the region. Additionally, the results represent a first step in understanding irrigation in Mato Grosso, showing immense potential for application in future studies.

Keywords: Center pivots; Remote sensing in agriculture; Water security.

RESUMO

SANTOS, Ana Beatriz dos, D.Sc., Universidade Federal de Viçosa, fevereiro de 2024 **Diagnóstico por sensoriamento remoto do uso dos recursos hídricos em regiões com intenso crescimento da irrigação no Brasil**. Orientador: Marcos Heil Costa. Coorientador: Everardo Chartuni Mantovani.

A irrigação por pivô central tem liderado o crescimento da irrigação no Brasil nos últimos anos. Contudo, a intensificação dos efeitos das mudanças climáticas pode levar a problemas em regiões altamente ocupadas por pivôs centrais. A redução do volume de precipitação ou da duração da estação seca gera frequentemente conflitos sobre o uso da água entre irrigantes e outros usuários. Portanto, é fundamental formular um diagnóstico da situação hidrológica nessas regiões. Este estudo selecionou três regiões brasileiras com intensa expansão da irrigação: as bacias dos Rios Corrente e Grande na Bahia, e o Alto Rio das Mortes no Mato Grosso. Embora sejam consideradas áreas com alto nível de tecnologia, não existe ainda uma rede sistemática de medição do uso da água. Os produtos de sensoriamento remoto permitem a estimativa da demanda de água do pivô central por meio da evapotranspiração (ET). Para as bacias dos rios Corrente e Grande, foi usado o produto de ET MODIS (produto MOD16A2 Versão 6 Evapotranspiration / Latent Heat Flux) para identificar sub-bacias com maior risco de conflitos hídricos. Depois de comparar a demanda estimada de água para irrigação com os dados da vazão do rio, três sub-bacias demonstraram uma situação potencialmente crítica relativamente à utilização dos recursos hídricos. Uma análise aprofundada destas sub-bacias também revelou que o uso de água pelos pivôs centrais tem aumentado constantemente ao longo dos anos, levando o consumo de água ao seu limite. Além do produto MODIS, outro banco de dados foi aplicado para estimar a irrigação por pivôs centrais, o conjunto de dados de evapotranspiração diária fornecido pela plataforma GLODET para o Alto Rio das Mortes. Além disso, dados de ET medidos via covariância de vórtices turbulentos foram utilizados para avaliar a precisão dos dois produtos. Os resultados mostraram que o novo conjunto de dados de ET apresentou melhorias em comparação com a versão anterior utilizada, que subestima a ET na região. Além disso, os resultados representam um primeiro passo no entendimento da irrigação em Mato Grosso, mostrando grande potencial para aplicação em estudos futuros.

Palavras-chave: Pivôs centrais; Sensoriamento remoto na agricultura; Segurança hídrica.

LIST OF ILLUSTRATIONS

General Introduction

Chapter 1

Chapter 2

LIST OF TABLES

Chapter 1

Chapter 2

SUMMARY

General Introduction

In 2023, the Brazilian grain production set a record by reaching 322 million tons, marking an 18% increase compared to the total production in 2022 (272 million tons). Brazilian agriculture's success highlights local producers' dedicated efforts and underscores the abundant resources available in the country. Brazil has a sizable portion of its territory under a tropical climate. With no limitations imposed by temperature and radiation, two harvests are feasible in regions with around 200 or more days of precipitation per year (Costa et al., 2019). Additionally, abundant water resources make irrigation viable, used to enhance productivity and even as an alternative means to enable a second crop in a year (ANA, 2021).

Irrigation requires investment and technology for its application. Among the various existing practices, center pivot irrigation presents satisfactory results in productivity with a satisfactory level of efficiency in the use of water resources (Mantovani, 2009). According to the latest Irrigation Atlas produced by ANA (ANA, 2021), this typology leads irrigation growth in recent years in Brazil. In 2017, around 1,556 Mha were irrigated by center pivots, an area 50 times larger than that mapped in 1985 (ANA, 2021). Furthermore, the concentration of center pivots occurs in well-defined centers, notably in the states of Minas Gerais (28.8%), Goiás (17.3%), São Paulo (14.6%), Bahia (14.0%), Rio Grande do Sul (9.3%) and Mato Grosso (8.7%) (ANA, 2021).

However, the uncontrolled growth of irrigation systems in a basin may lead to sustainability issues for water resource users. Climate changes projected for the future already point to a tendency to reduce rainfall in some regions in Brazil (Hofmann et al., 2023; Leite-Filho et al., 2021; Pereira et al., 2022). For the Cerrado, the biome with the highest concentration of center pivots currently (65%, ANA, 2021), it is estimated that the duration, intensity, and frequency of meteorological and hydrological droughts are expected to increase

in the coming years in some regions (Rodrigues et al., 2019). The decrease in rainfall can have impacts on irrigation, including a reduction in river flow (Salmona et al., 2023) and also in groundwater-based river flow regulation during dry periods (Pereira et al., 2022; Cambraia Neto et al., 2021). According to Salmona et al. (2023), a total water reduction of 23,653 m^3/s is expected by 2050, equivalent to a decrease of 33.9% in river flows in the Cerrado. Prolonged dry periods can increase the frequency and amount of water applied via irrigation, which may lead to conflicts between irrigators and the other water users in highly irrigated basins.

Conflicts are emerging in regions heavily dominated by center pivots. According to the National Water Agency, currently, approximately 28 areas in Brazil have been identified as highly occupied by irrigation, designated by the agency as "irrigation zones" (ANA, 2021). In Western Bahia, the irrigation zone characterized by the Corrente and Grande basins (Figure 1) is already facing these conflict situations (Pousa et al., 2019). A notable case occurred in 2017 in the city of Correntina, within the Corrente River basin, when citizens revolted against the presence of irrigators, resulting in the invasion of farms and the loss of equipment (Pousa et al., 2019). In addition to the Corrente River basin, the Grande River basin also faces significant challenges due to the large number of center pivots and a history of conflicts.

As occurs in Bahia, irrigators in the Alto Rio das Mortes irrigation zone, referred here as RM, located in Mato Grosso (Figure 1), have been under pressure to find solutions that allow the expansion of irrigation without generating conflicts over water use. The region has around 9% of its territory already occupied by center pivots (ANA, 2021). Furthermore, data from the National Water Agency (ANA, 2021) inform that the abundance of fresh water and the great suitability of soil and relief favor the expansion of irrigated agriculture in the region.

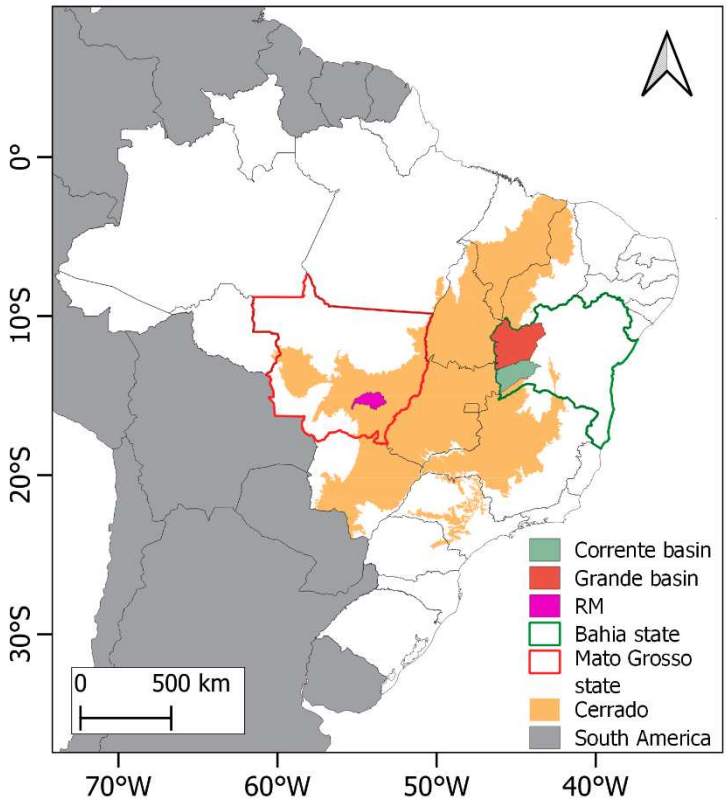

Figure 1. Location of study regions. Corrente and Grande basin located in the Western part of Bahia state; and RM (Alto Rio das Mortes irrigation zone) located in the Southeast of Mato Grosso state.

Considering the context of irrigation expansion and climate instability, it is important to formulate a diagnosis of the water situation in these regions. Although these are areas with high technological level in the field, there is no systematic measurement network for water use by center pivots. Such a monitoring system will allow a more confident and sustainable regional management of irrigated agriculture, maximizing the use of water resources, food production, and economic development, while reducing the risk of water conflicts (Pousa et al., 2019). Therefore, it is necessary to develop a methodology for indirectly measuring the demand for water resources for irrigation.

Remote sensing is consolidated and widely used in mapping irrigated areas (Bazzi et al., 2019; Pun et al., 2017; Saraiva et al., 2020). However, estimating the amount of water used for

irrigation is a much more complex task (Jalilvand et al., 2019). Over the years, studies have investigated different methodologies for obtaining water demand for crops (Mu et al., 2013; Neale et al., 2012; Norman et al., 1995). Despite different methodologies and limitations, the studies were able to capture general irrigation patterns, affirming the potential use of remote sensing to calculate water consumption in irrigated agriculture. Therefore, the development of a methodology that uses indirect measurements of water demand for crops can be of major help in regions with a high concentration of pivots. By combining estimates of water demand for irrigation with the availability of surface water resources, it is possible to diagnose the use of water resources in the basins, helping government and irrigators in decision-making.

This thesis has the goal of using remote sensing data to diagnose water resources in regions experiencing intensive expansion of irrigation in Brazil. It is divided into two chapters. In the first chapter, I investigate the irrigation scenario in Western Bahia by assessing water usage by irrigation in the Corrente and Grande River basins. This investigation involves developing a method to estimate irrigation demand using an evapotranspiration remote sensing product, the MOD16A2 product from the MODIS Global Evapotranspiration Project. The final diagnostic of water conflict situation is made by using river gauge data. In the second chapter, I explore the potential application of a new evapotranspiration product in estimating irrigation demand in the RM irrigation zone. In this study, I incorporate measured evapotranspiration data from an eddy covariance tower to evaluate the advantages and disadvantages of the new product in comparison to the MODIS product.

Chapter 1: Remote sensing diagnosis of water use and water stress in a region with intense irrigation growth in Brazil.

Santos, A. B., Costa, M. H., Mantovani, E. C., Boninsenha, I., & Castro, M. (2020). A remote sensing diagnosis of water use and water stress in a region with intense irrigation growth in Brazil. *Remote Sensing*, 12(22), 3725.

Abstract

Western Bahia, Brazil, is a classic example of a region where intense irrigation growth has led to acute water stress situations in a few small basins. The water stress problem has the potential to grow regionally. However, there are currently no systematic field measurements of water withdrawn from rivers or groundwater to supply irrigation systems. In this work, we merge remote sensing and river gauge data to assess both the amount of water used for irrigation in Western Bahia and also its consequences for regional water stress, identifying water conflict situations and assessing water security. Remote sensing products used include time series of the normalized difference vegetation index, evapotranspiration, and rainfall. Field data include time series of river discharge and calibration data for crop status and actual evapotranspiration. From calibrated remote sensing products, three-day water balances were calculated for each center pivot using computations of irrigation depth and water uptake for irrigation, both individually at the center-pivot scale and integrated regionally. From these regional integrations, a simple water-use diagnostic indicated that three sub-basins presented the most critical conditions for water conflicts. An in-depth analysis of these sub-basins shows that, despite the high-water stress, water use for irrigation has been steadily increasing, pushing the water use to its limits. This work demonstrates that the use of remote sensing products together with field data is a powerful tool for diagnosing water conflict situations. The limitations of this work relate to the absence of field data to validate the water uptake estimated and to the lack of

additional long-term and high-quality river flow stations to provide diagnostics for all small basins in the region.

1.1 Introduction

The irrigated area in Brazil has more than doubled from 3.1 Mha in 1996 to 6.9 Mha in 2015 (ANA, 2017). This increase was concentrated in a few regions that provided excellent conditions for agricultural growth, such as flat topography, availability of surface water and groundwater, and power infrastructure. One of these regions is the western part of the state of Bahia (Figure 1.1). Irrigation in this region increased by 150-fold from 1985 to 2016 (ANA, 2017), and a 90% increase was reported in just eight years, from 2010 to 2018 (Pousa et al., 2019).

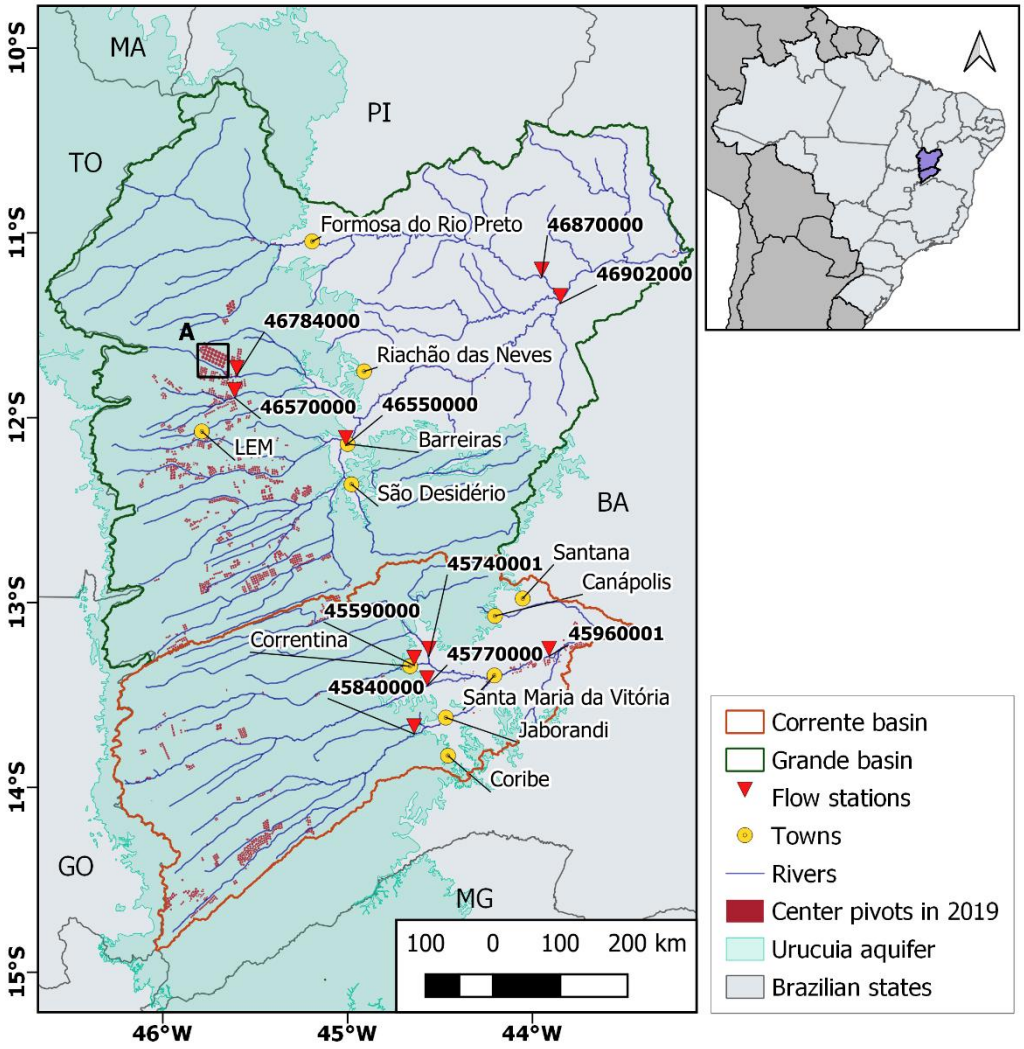

Figure 1. 1 Study area, main towns, and basins in Western Bahia. Red triangles and station code numbers mark the flow stations analyzed, and yellow circles indicate the region's main towns. LEM is the town of Luis Eduardo Magalhães. The rectangle (A) represents the area detailed in Figure 3 (c) and (d). The Urucuia aquifer is also a source of groundwater for irrigation. MA, TO, PI, GO, and MG refer to Brazilian states adjacent to Bahia (BA).

Along with the intense growth of the irrigated area, analyses of hydroclimatic time series for the period 1978–2015 indicated statistically significant reductions in rainfall (Pousa et al., 2019), groundwater levels (Marques et al., 2020), and river discharge in some flow stations (Pousa et al., 2019). The combination of reduced availability and increased demand for water resources suggests that, if current trends are maintained, conflicts over water may become more

frequent in the next years or decades. A monitoring system in which the availability and demand for water resources for irrigation are measured and monitored is a first step to provide water security to this region (Pousa et al., 2019).

Although remote sensing has been widely used to map irrigated areas using several techniques (Bazzi et al., 2019; Pun et al., 2017; Saraiva et al., 2020), estimation of the amount of water used for irrigation by remote sensing is a much more complex task (Jalilvand et al., 2019). Over the years, many studies have investigated the use of optical sensors, including Landsat (Folhes et al., 2009; Peña-Arancibia et al., 2014) and MODIS (Moderate Resolution Imaging Spectroradiometer, Peña-Arancibia et al., 2016), to quantify water use for irrigation. Despite the different methodologies and limitations, the studies could capture overall irrigation patterns, affirming the potential use of remote sensing to calculate water consumption in irrigated agriculture.

There are currently no systematic field measurements of water withdrawn from rivers or groundwater in Western Bahia. I hypothesize that remote sensing data can fill this data void. Therefore, the main objective of this work is to provide estimates of water uptake for irrigation using remote sensing products. For the period 2001 to 2019, I map all center pivots in the region, determine their status as irrigated or non irrigated, and estimate the monthly irrigation depth applied by a water balance equation using products for evapotranspiration (ET; from the MOD16A2 product of the MODIS Global Evapotranspiration Project) and precipitation (from the Tropical Rainfall Measuring Mission (TRMM) 3B42 product) as inputs. I also use field data for planting and harvest dates and actual evapotranspiration collected from 69 center pivots to calibrate the ET from the MOD16A2 product. Then, I determine the actual irrigated area and the water uptake for irrigation (Qi), which is aggregated for the drainage area of selected fluviometric stations.

I also merge remote sensing and river gauge data to assess not only the amount of water used for irrigation in Western Bahia but also its consequences for the water stress of the region, and we identify water conflict situations and assess water security in selected basins. The study focuses on ten representative sub-basins delimited from flow stations with high-quality data. Five of them are in the Corrente basin, and five are located in the Grande basin (Figure 1), the two largest basins of the region. For these, I provide a water use diagnostic using simple environmental indicators, and for the three sub-basins that exhibited the most critical conditions, I present an in-depth analysis of the 2001–2019 data time series produced here.

1.2 Materials and Methods

1.2.1 Remote Sensing data

To quantify the actual irrigated area, I used two normalized difference vegetation index (NDVI) data sets. First, imagery from Landsat 5, 7, and 8 was used to calculate the NDVI. The missing pixels (those affected by clouds or cloud shadows) were filled using the MODIS MOD13Q1 NDVI product Version 6. This data set is a 16-day composite and provides vegetation index values on a per-pixel basis with a spatial resolution of 250 m. MODIS NDVI pixels are computed from atmospherically corrected bi-directional surface reflectance and represent the best pixel result of a 16-day composite. Then, both Landsat and MODIS data are filtered using the irrigated land mask.

The MODIS ET data set (MOD16A2 Version 6 Evapotranspiration/Latent Heat Flux product) was used to estimate actual evapotranspiration. The algorithm is based on the logic of the Penman–Monteith equation, and it includes inputs of daily meteorological reanalysis data along with other MODIS remotely sensed data products, such as dynamical vegetation optical properties, albedo, and land cover (Mu et al., 2013). The MOD16A2 data set is an eight-day

composite product; i.e., the pixel values for the evapotranspiration layer are the sum of all eight days within the composite period. The product is available at 500 m pixel resolution for the entire global vegetated land surface.

Daily precipitation products were used to calculate the water balance and to estimate water uptake for irrigation. We used the daily accumulated product generated from the research-quality three-hourly TRMM Multi-Satellite Precipitation Analysis (TMPA, product 3B42, GESDISC, 2020). The TRMM data set provides a calibration-based sequential scheme for combining precipitation estimates from multiple satellites and is available at a 27.75 km pixel resolution.

1.2.2 Field Actual Evapotranspiration Data

Field data of actual evapotranspiration (ET_a) was used to calibrate the remote sensing ET product. The field data include daily evapotranspiration values of 69 center pivots during the years 2017 and 2018, in a total of 338 pivot-months of data (an average of 4.9 months per pivot). Crops cultivated included soybean (*Glycine max*), maize (*Zea mays*), common bean (*Phaseolus vulgaris*), and cotton (*Gossypium hirsutum L.*). ET_a was calculated using the classic FAO 56 methodology (Allen et al., 1998), in which $ET_a = K_s\ K_L\ K_c\ ET_o$, where reference evapotranspiration (ET_o) is calculated using the standard Penman–Monteith approach (Allen et al., 1998), using daily data measured at automatic weather stations (temperature, relative humidity, wind speed, and solar radiation); the crop coefficient K_c is a function of the crop and its stage of development; K_s refers to the wetting frequency; and the landscape coefficient K_L refers to the method of irrigation (Bernado, n.d.; Mantovani, 2009). This methodology is part of the Valley Scheduling software (used by the Irriger Connect platform), which provides routine irrigation management services to the selected center pivots.

1.2.3 River Flow Data

River flow data was used to estimate the surface water resources available. The daily river flow data used were obtained from ANA, the Brazilian Water Agency. I selected five fluviometric stations for each study basin (Table 1.1) according to the characteristics of their area upstream (sub-basin). First, I selected stations with a large area upstream to provide a regional perspective for the basins of Corrente (station code 45960001) and Grande (46902000). Second, I selected stations that have a high percentage (>4%) of the area upstream used for irrigation (45840000, 46570000, and 46784000′). Finally, I selected stations that experienced a recent expansion in the irrigated area (45590000, 45740001, 45770000, 46550000, and 46870000). All station data series have at least 30 years of data except station 46784000′. Detailed information about the stations, their locations, and their drainage areas are shown in Table 1.1, Figure 1.1, and Figure 1.2, respectively.

Table 1.1 Selected fluviometric stations used in this study. The prime (′) after the Rio Branco station (46784000′) indicates that the irrigated area upstream is in an area larger than the actual drainage area. The percentage of irrigated area is given with respect to the drainage area upstream or, in the case of 46784000′ (+), with respect to the area of the region that is irrigated using water from the Rio Branco.

Basin	Station Code	River	Station Name	Drainage Area, km²	Irrigated Area Upstream in 2019, km² (%)	Times Series	
						Begin	End
Corrente	45590000	Rio Correntina	Correntina	3852.4	65.4 (1.7%)	1978	2017
	45740001	Rio do Meio	Mocambo	9039.3	91.2 (1.0%)	1978	2017
	45770000	Rio Arrojado	Arrojado	5644.5	33.2 (0.6%)	1978	2017
	45840000	Rio Formoso	Gatos	7132.7	295.0 (4.1%)	1978	2017
	45960001	Rio Corrente	Porto Novo	31,155.7	517.0 (1.7%)	1978	2017
Grande	46550000	Rio Grande	Barreiras	24,495.8	776.4 (3.2%)	1978	2017
	46570000	Rio de Janeiro	Ponte Serafim	2521.8	120.1 (4.8%)	1978	2017
	46784000	Rio Branco	Savana	685.0	117.1 (17.1%)	2003	2017
	46784000′	Rio Branco	Savana	1041.3⁺	195.3 (18.7%)	2003	2017
	46870000	Rio Preto	Faz. Porto Limpo	22,151.0	39.1 (0.2%)	1978	2017
	46902000	Rio Grande	Boqueirão	46,395.7	1158.3 (2.5%)	1978	2017

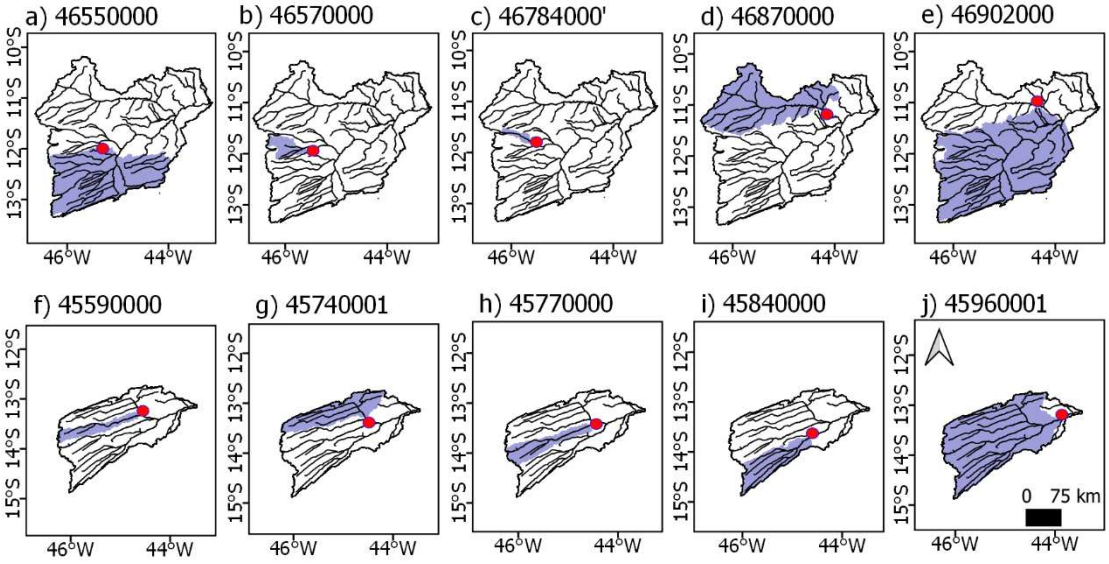

Figure 1.2 Delimitation of study sub-basins. The Grande sub-basins, identified by fluviometric station code, are: (a) 46550000; (b) 46570000; (c) 46784000'; (d) 46870000; and (e) 46902000. The Corrente sub-basins are: (f) 45590000; (g) 45740001; (h) 45770000; (i) 45840000; and (j) 45960001. The red dots represent the locations of the fluviometric stations.

1.2.4 Computation of Irrigated Area

The starting point for computing irrigated areas in the region is the center pivot maps developed by Pousa et al. (2019). This data set was produced using a four-step procedure that included (i) processing imagery from Landsat 5, 7, and 8 using the Google Earth Engine cloud to mosaic the images for the region and filter the pixels first for the dry period (April to September) and later for the NDVI median of the study region; (ii) merging the filtered map with other center pivot maps to produce an initial map for the region; (iii) removing duplicated features and topology errors; and (iv) validating positional accuracy through a trend and precision analysis to produce a final map without trends in center pivot sizes and locations with accuracy adequate to the scale of 1:150,000 that is compatible with the resolution of the Landsat images. More details on the methodology can be found in (Pousa et al., 2019). This data set,

however, should be considered a data set of available infrastructure for irrigation, as it does not inform when there is a crop on the field that is being irrigated. The initial data set was produced for 1990–2018, but in this work, we updated the time series to 2019. Due to the need to cross-analyze the data against several MODIS products, I use data only from 2001 to 2019.

The identification of the actual growing seasons for each center pivot is fundamental for understanding the water demand. Thus, a simple classification of center pivots was performed based on the presence or absence of a growing crop.

NDVI has been shown to be a useful indicator of spatial-temporal changes in vegetation growth and distribution over time (Barbosa et al., 2006; Pereira et al., 2018). Due to its ease of application and reliable results, NDVI is perhaps the most widely used vegetation index in remote sensing studies (Karthikeyan et al., 2020). I classified the center pivots into two classes (growing crop/no crop) using the NDVI. First, I calculated the NDVI using all Landsat data available for the two basins. Next, I made monthly composites with pixels that had the maximum value of NDVI and eliminated the missing data due to clouds or cloud shadows. I then filled the gaps in the Landsat NDVI composite with the same composite for MOD13 NDVI data. Figure 1.3a shows an example of the filled time series for one center pivot.

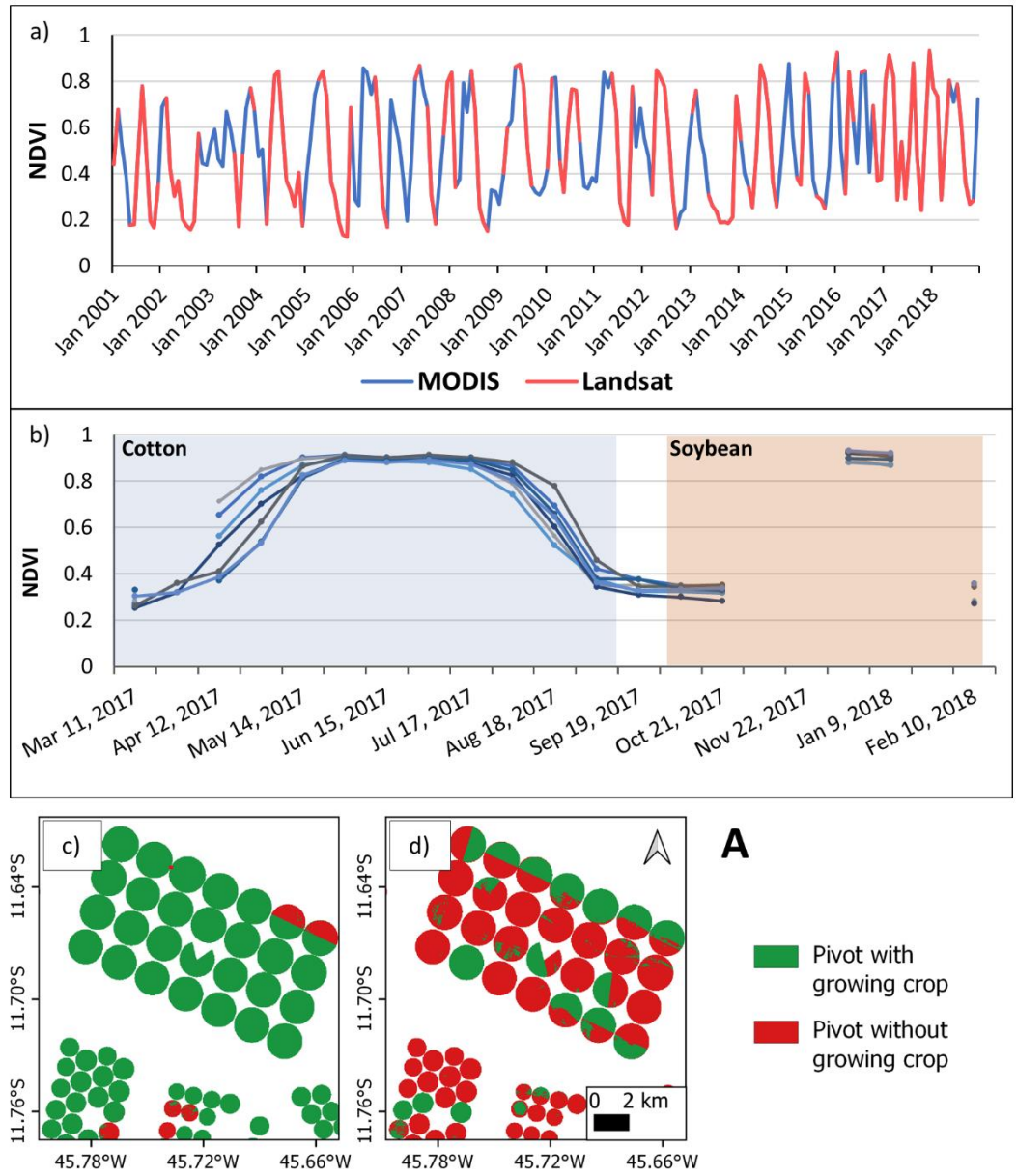

Figure 1. 3 Normalized difference vegetation index (NDVI) analyses and classification of center pivots: (a) an NDVI series produced from Landsat data filled with NDVI series from MODIS MOD13 data for a single sample pivot; (b) NDVI behavior in seven example center pivots in the Corrente basin, where shaded areas indicate periods when a crop was on the field, according to field work; (c) final classification of center pivots in May 2017 for the rectangle marked A in Figure 1.1; (d) final classification of center pivots in September 2017, also for rectangle A. Panels (c) and (d) show some pivots being fully irrigated, some being half-irrigated, and some not being irrigated.

To determine the NDVI threshold between a growing crop and no crop, we collected field data on the planting and harvest dates for 69 center pivots during the years 2017 and 2018. An example of (Landsat only) NDVI behavior in seven center pivots located in the Corrente basin is shown in Figure 1.3b. In this case, the seven pivots were each planted and harvested in the same week with the same crop. Between two crop rotations, NDVI values range from 0.25 to 0.35. Thus, I defined the NDVI value of 0.25 as the threshold between crops and no crops and applied this threshold for all monthly composites. Pixels with values higher than this limit were classified as pixels with a growing crop, and pixels with values lower than 0.25 as pixels without a growing crop. I identified two well-defined seasons, in one of which we expect to find higher demand for irrigation water and in the other, lower demand. The first season occurs between April and June (with a peak in May; Figure 1.3c) when most of the center pivots are in use. The second season, with the least crop cover, occurs between August and October (with a peak in September; Figure 1.3d) when most of the pivots do not have a growing crop. During the rainy season (November to March), irrigation is not expected to happen, except during long dry spells.

1.2.5 Computation of Actual Evapotranspiration, Irrigation Depth, and Water Uptake for Irrigation

To calculate ET_a for all center pivots in the region, we corrected the evapotranspiration from MOD16 data using field evapotranspiration data. First, I aggregated all MODIS ET pixels inside a center pivot, calculating a pivot average based on the proportion of area covered by each MODIS 500 m pixel within each pivot. Second, we calculated a regression line between the field ET_a and the aggregated MODIS ET (ET_{MODIS}) for the 338 pairs of pivot-months of data available. I tried adjusting both data sets at different time scales: 8-day, 16-day, and monthly. Monthly aggregated data yielded the best adjustment ($y = 0.9756x$, $R^2 = 0.987$, where $y = \log_{10} ET_a$ and $x = \log_{10} ET_{MODIS}$; ET_a and ET_{MODIS} are in mm month^{-1}. Then, I corrected all

monthly ET_{MODIS} estimates using this relationship, producing a monthly time series of ETa for each center pivot from January 2001 to December 2019.

The water application rate for each center pivot depends not only on ET_a but also on the local precipitation and the efficiency of water application by the irrigation system (Ɛ). Here I reproduce the methodology typically used by farmers in the field, closing the water balance of each center pivot in a three-day window and considering that irrigation occurs only when the amount of water lost by ET is greater than the input by precipitation. The corrected monthly ET_a data was considered uniform throughout the month; daily ET_a was obtained by the division of the monthly ET_a value by the number of days in the month. The irrigation depth (D)—or water application rate—was calculated according to Equation 1:

$$D(i) = \max\left(\frac{ET_a(i) - P(i)}{\varepsilon}, 0\right) \quad (1)$$

where P(i) is the three-day TRMM precipitation on pivot i and $ET_a(i)$ is its three-day evapotranspiration. The center pivot system used in the region is considered a highly efficient irrigation system, with efficiency ranging from 80%–90% (Bernado, n.d.; Coelho et al., 2005), so we adopted Ɛ = 0.85. When P(i) > $ET_a(i)$, the crop ET demand was fully satisfied by the precipitation, and there was no irrigation in the center pivot in that period, so D(i) = 0. Next, I accumulated the computed three-day water application rate monthly.

The water uptake for irrigation of each center pivot $Q_i(i)$ is just the product of the water application rate D(i), in mm month^{-1} by the area of the center pivot (ha), with units adjusted to $m^3\ s^{-1}$.

1.2.6 Integration of Results per Sub-Basin

This study presents water resources analysis by sub-basin, where a sub-basin is the drainage area upstream of the fluviometric stations in Table 1.1 and Figure 1.2. Individual pivot results were aggregated according to their position in the drainage area of each fluviometric station. I started this analysis with the integration of all variables calculated: precipitation, water application rate, actual irrigated area, water uptake for irrigation, measured river discharge, and naturalized flow (explained below).

To give an overview of the precipitation regime for each basin, we aggregated the daily data and calculated the monthly mean. The average water application rate by sub-basin, in mm month^{-1}, was calculated by weighting the individual pivot values of D(i) by pivot area. During this procedure, we also calculated the actual irrigated area by sub-basin, which was the sum of the pivot areas that had monthly D(i) greater than zero. The accumulated water application rate Q_i is the sum of the individual $Q_i(i)$ across the drainage area of the fluviometric station.

In addition to the measured river discharge in each station (Q), I also calculated "naturalized flows" series for each river at each station. The naturalized flow (Q*) is the corresponding flow that would occur in a river section if there were no anthropic actions in the drainage area contributing to the section. The naturalized series are synthetic series created to reproduce the original flow of the river through the return of the water used for irrigation back to the river, i.e., $Q^* = Q + Q_i$. Q_i is available only since 2001, so I could only calculate naturalized flows for this period.

1.2.7 Data Analysis

To assess the irrigation impact for each sub-basin, I analyze the occurrence of two possible critical water resource conditions related to the maximum water uptake for irrigation during 2001–2019 (Q_{imax}) and the minimum river flow (Q_{min}). For the analysis of the first

condition, the state of Bahia adopts the criterion of 80% of Q_{90} as the limit of surface water flow that can be granted for human use (State Decree 6296 of 21 March, 1997). Q_{90} is the flow expected to be present in the river at least 90% of the time. In this study, I use the value Q_{90}*, calculated using Q*. Thus, in the scenario that Q_{imax} exceeds 80% of Q_{90}*, then irrigation would create a water use conflict situation, i.e., the water demand for irrigation would exceed the availability of water resources.

The other critical condition is related to the minimum discharge. If 80% of Q_{90}* is the maximum allowable to be allocated, then 20% of Q_{90} is the minimum discharge needed to maintain the ecological functions of the river. Thus, a ratio Qmin/Q90* that is less than 20% characterizes a condition of water insecurity.

1.3 Results

1.3.1 Water Use Conflicts and Water Insecurity

This section presents an overview of the impact of water resources in all ten sub-basins. According to our results, the conditions in the Corrente sub-basins are the most comfortable with respect to water availability. None of these sub-basins shows detectable indications of water conflict or water insecurity (Table 1.2). All sub-basins show low Q_{imax}/Q_{90}* values (maximum value is 16.3%; critical limit is 80%). In addition, the similar values of Q_{90} and Q_{90}* indicate small Q_i amounts withdrawn from the rivers during the low-flow season. Although there is a large area with irrigation in the 45840000 sub-basin (4.1%, see Table 1.2), the low Q_{imax}/Q_{90}* ratio (16.3%) suggests a low demand for water resources by irrigation. Moreover, as irrigation expansion in the basin is recent, the operation of many recent center pivots did not affect most of the Q* series.

Table 1. 2 Results for maximum irrigation water update (Q_{imax}), river flow expected to be present at least 90% of the time (Q_{90}), the naturalized flow that would have been expected to be present at least 90% of the time (Q_{90}*), Q_{imax}/Q_{90}*, minimum river flow (Q_{min}), and Q_{min}/Q_{90}* for all sub-basins analyzed. Critical conditions are defined as: Q_{imax}/Q_{90}* > 80% and Q_{min}/Q_{90}* < 20%.

Basin	Station Code	Q_{imax} ($m^3\ s^{-1}$)	Q_{90} ($m^3\ s^{-1}$)	Q_{90}* ($m^3\ s^{-1}$)	Q_{imax}/Q_{90}* (%)	Q_{min} ($m^3\ s^{-1}$)	Q_{min}/Q_{90}* (%)
Corrente	45590000	1.91	23.00	23.15	8.3	19.19	82.9
	45740001	2.73	24.51	24.82	11.0	18.47	74.4
	45770000	1.08	42.99	42.99	2.5	31.14	72.4
	45840000	8.84	53.11	54.35	16.3	37.10	68.3
	45960001	15.18	135.83	138.66	10.9	104.25	75.2
Grande	46550000	29.83	54.80	59.25	50.3	24.60	41.5
	46570000	5.73	5.99	7.10	80.7	2.62	36.9
	46784000′	7.72	7.19	9.29	83.1	3.82	41.1
	46870000	1.38	74.97	75.04	1.8	63.75	84.9
	46902000	46.05	187.96	194.17	23.7	146.58	75.5

Q_{90} and Q_{90}* were calculated for the period 1978–2017 for all flow stations, except for 46784000′, where the period was 2003–2017.

For the Grande basin (Table 1.2), we identify water conflict situations in the two smallest sub-basins — 46570000 (Rio de Janeiro) and 46784000′ (Rio Branco) — both with drainage areas less than 2600 km2 (see Table 1.1 for drainage areas). Both sub-basins present a remarkably high concentration of irrigated areas: 4.8% in Rio de Janeiro and 18.7% in the Rio Branco (Table 1.1). Q_{imax} reaches 80.7% of Q_{90}* in the 46570000 sub-basin and 83.1% of Q_{90}* in the 46784000′ sub-basin. The difference between Q_{90} and Q_{90}* is also high in these two basins: 1.11 m3 s−1 (18.5%) in Rio de Janeiro and 2.10 m3 s−1 (29.2%) in Rio Branco. This difference indicates that there is persistent use of irrigation (high Q_i values) during the low-flow season. Despite the water conflict situation, in both sub-basins, the minimum discharge ratios recorded were well above the 20% of Q_{90}* minimum limit that would characterize water insecurity (36.9% in the Rio de Janeiro and 41.1% in the Rio Branco). The 46550000 sub-basin

(Rio Grande at Barreiras) also deserves attention. Although it is not formally experiencing water conflict as defined above, the high Q_{imax}/Q_{90}* ratio (50.3%) is an alert regarding the irrigation expansion in the region. This sub-basin includes all the Upper Rio Grande basin, including the Rio das Ondas, but does not include the Rio de Janeiro and Rio Branco. It is also important to note that the minimum flow at sub-basin 46550000 is 41.5% of Q_{90}*, which is similar to 46570000 (36.9%) and 46784000′ (41.1%).

In summary, three sub-basins stand out as presenting reason for concern: 46550000, 46570000, and 46784000′. Therefore, I also conducted an in-depth investigation to analyze changes in irrigation and other relevant data throughout the period 2001–2019 in these sub-basins.

1.3.2 Integrated Results for Selected Critical Basins

Figure 1.4 shows the results for the 46550000 sub-basin, the Rio Grande at Barreiras. The monthly precipitation pattern observed is representative of the regional climate, with two well-defined seasons: rainy (October to April) and dry (May to September; Figure 1.4a). The monthly precipitation presents substantial variability, ranging from 0 to ~450 mm month–1. The same precipitation pattern is observed in the other critical basins.

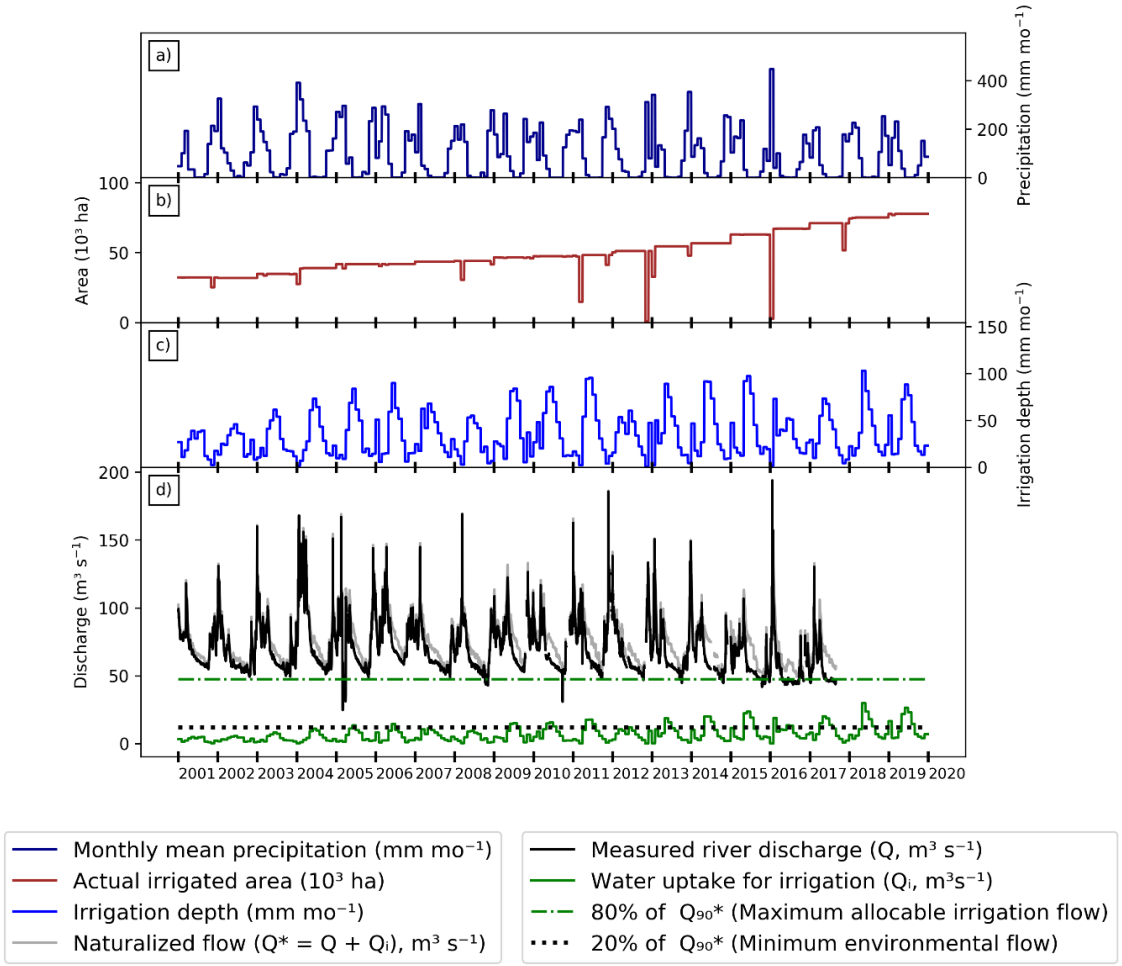

Figure 1. 4 Integrated results of flow station 46550000 in the Grande basin: (a) monthly average precipitation series from 2001 to 2019; (b) actual irrigated area per month from 2001 to 2019; (c) monthly irrigation depth from 2001 to 2019; (d) measured (Q) and naturalized (Q*) river discharge and irrigation uptake (Q_i), where $Q^* = Q + Q_i$. The green and black dashed lines represent the minimum environmental flow and maximum allocable irrigation flow, respectively.

Figure 1.4b shows that the actual irrigated area increased from 32,000 ha in 2001 to 77,000 ha in 2019, following the increase in center pivots from 318 in 2001 to 766 in 2019. In addition, the stability of the irrigated area over the months indicates that the irrigation systems operate throughout the entire year, with interruptions only in a few high-rain months. On the

other hand, the average irrigation depth presents substantial seasonal variation, ranging from <10 mm month^{-1} in the rainy season to ~100 mm month^{-1} in the dry season (Figure 1.4c).

Figure 1.4d presents the environmental impact of irrigation. The Rio Grande has a seasonal flow consistent with the rainfall pattern, with peaks in the rainy seasons and lows in the dry seasons. In this figure, a water insecurity condition would be characterized by the solid black lines being below the dotted black line ($Q_{min} < 0.2 \cdot Q_{90}$*). In comparison, the solid green line going above the dot-dashed green line ($Q_i > 0.8 \cdot Q_{90}$) characterizes a water conflict situation. As we observed earlier, there is no water use conflict or insecurity situation in this sub-basin. The irrigation discharge did not exceed 80% of Q_{90}* in any month of the period, but the Q_i values have been steadily increasing and reached the maximum value for the series in June 2018 (Q_i = 29.83 m^3 s^{-1}, 50.3% of Q_{90}*).

Overall, the actual situation for 46550000 does not seem to be critical in comparison to the two basins discussed below. However, the growing irrigation trend requires attention for management agencies and farmers to avoid water conflicts in the future. Moreover, the large size of this sub-basin (24,500 km^2) suggests that localized problems may be occurring in smaller sub-basins, as in the cases of Rio de Janeiro and Rio Branco.

The Rio de Janeiro sub-basin upstream of 46570000 is much more water-stressed (Figure 1.5; water insecurity and water conflict conditions are interpreted as in Figure 1.4). This sub-basin has had remarkably high irrigation since the 1990s (Pousa et al., 2019). Currently 12,100 ha of irrigation systems are installed in this sub-basin, and nearly all are in use every month (Figure 1.5b). In 2005, Q_i reached 4.33 m^3 s^{-1}, 60.8% of Q_{90}*, and yet from 2005 to 2019, the number of center pivots increased by 18.6%, and the actual irrigated area increased from 10,287 to 12,011 ha (Figure 1.5b). This expansion pushed water use past the threshold of a conflict situation, with Q_i setting new records repeatedly (4.63 m^3 s^{-1} in 2010, 5.19 m^3 s^{-1} in 2015) and finally reaching 5.73 m^3 s^{-1} (80.7% of Q_{90}*) in May 2018 (Figure 1.5d; Table 1.2).

Q_i also remained high during the dry season throughout the period, showing that the irrigation activity has been near the limit since 2005.

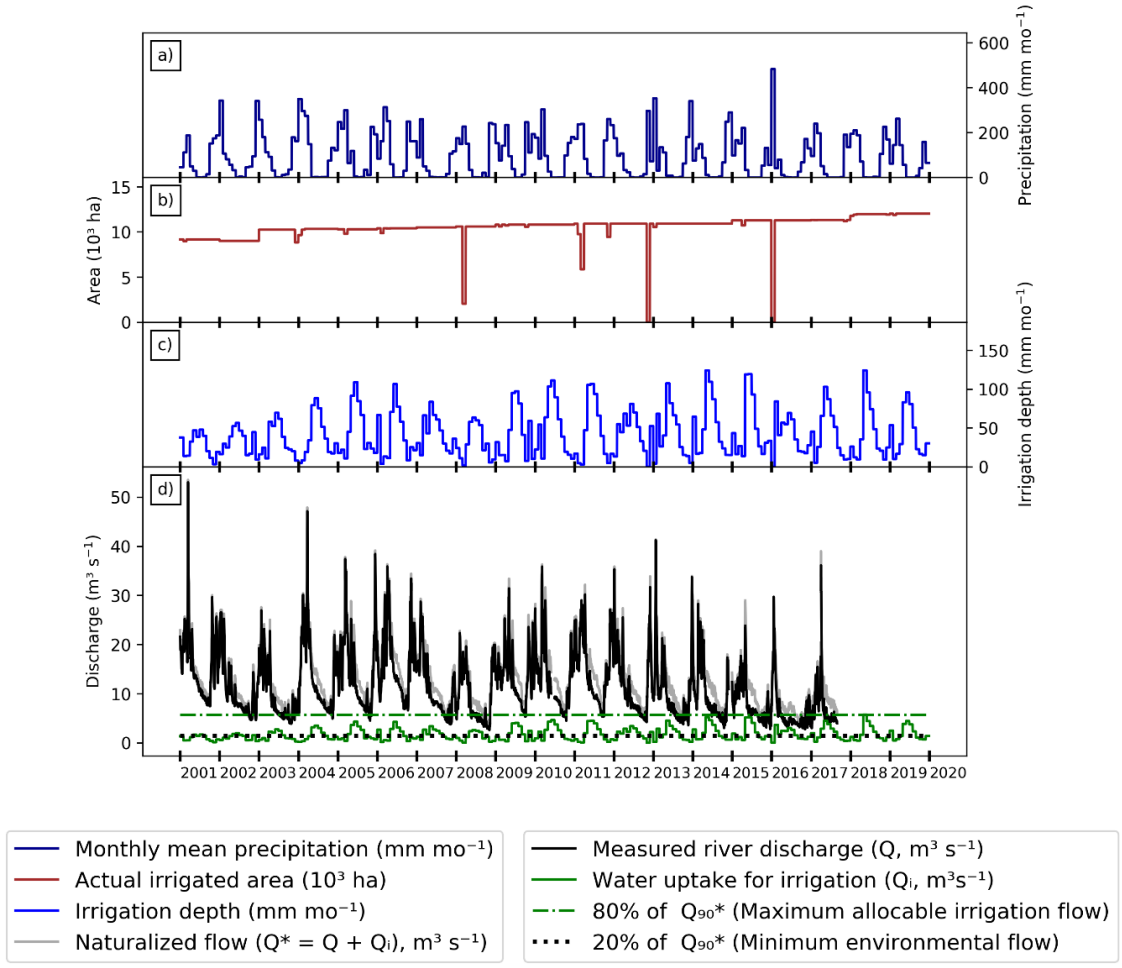

Figure 1. 5 Integrated results of flow station 46570000 in the Grande basin: (a) monthly average precipitation series from 2001 to 2019; (b) actual irrigated area per month from 2001 to 2019; (c) monthly irrigation depth from 2001 to 2019; (d) measured (Q) and naturalized (Q*) river discharge and irrigation uptake (Q_i), where $Q^* = Q + Q_i$. The green and black dashed lines represent the minimum environmental flow and maximum allocable irrigation flow, respectively.

Nevertheless, the imminence of water uses conflicts in the Rio de Janeiro sub-basin since 2005 might have discouraged the installation of new center pivots in the following years, explaining the relatively small growth rate of irrigation systems when compared to the Rio

Branco or even the larger Rio Grande. Despite these critical Q_i values, Q is never less than the minimum environmental flow (20% of Q_{90}*) at any moment in the period. This apparent discrepancy may be explained by the fact that some of the irrigation pumps groundwater, not surface water. Although we are not able to infer from remote sensing data the source of the water pumped for irrigation, a quick analysis of water use grants issued from 2015 to 2020 indicates that grants for surface water use represent 94% of the total grants in this region.

It is no coincidence that the condition of sub-basin 46570000 is more critical than that of sub-basin 46550000. The larger drainage area upstream of the 46550000 station aggregates many tributaries, which obscures the potentially acute situations of smaller sub-basins. Small upstream drainage areas with a high density of irrigation systems are thus serious candidates for water conflicts.

This is clearly observed in sub-basin 46784000′, the smallest among all the analyzed basins, with an actual drainage area of only 685 km^2 (68,500 ha), which presents the most alarming scenario. The sub-basin is so small that a different type of analysis was necessary. By analyzing not only the irrigated area inside the drainage area but also the farm limits, we realized that a reasonable amount of irrigated area that depends on the waters of the Rio Branco is actually located outside its drainage area (Figure 1.6). For this reason, we redefined the contour of the region that is irrigated using water from the Rio Branco to provide a more realistic picture of what happens in the sub-basin. The region delimited by this new contour is hereafter referred to as 46784000´ and has a total area of 1041.3 km^2, of which 195.3 km^2 (19,530 ha; 18.7%) are irrigated. This is the highest density of irrigation systems for basins with water flow measurements in Western Bahia.

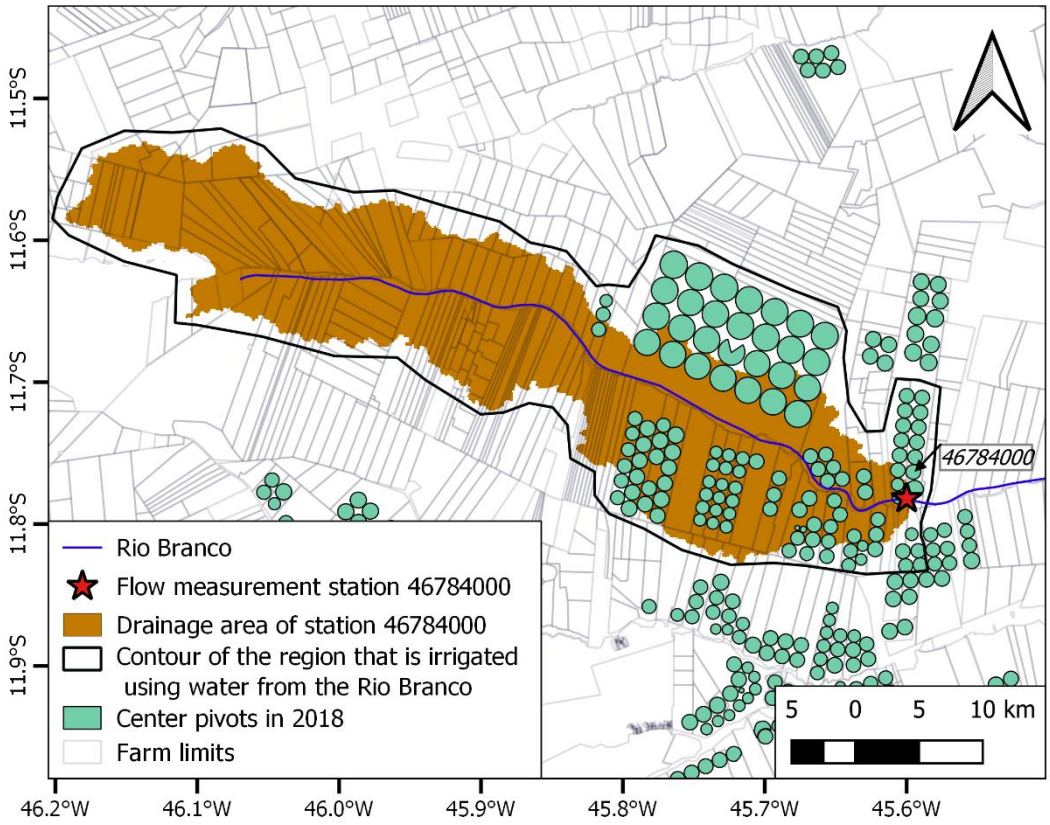

Figure 1. 6 Detail of the drainage area upstream of flow station 46784000 on the Rio Branco. The figure shows the locations of the center pivots in 2018 and the location of the flow station. The contour of Table 46784000. was drawn based on an analysis of the respective farm limits and the presence of irrigated areas.

Figure 1.7 shows the results for basin 46784000′ (water insecurity and water conflict conditions are interpreted as in Figures 1.4 and 1.5). While the behavior of seasonal precipitation and irrigation depth are similar to that of the two previously discussed sub-basins (Figure 1.7a,c), the actual irrigated area increased by 375%, from ~4100 ha in 2001 to ~19,500 ha in 2019 (Figure 1.7b), reaching 18.7% of the area of 46784000´, but even more astonishingly, 28.5% of the actual drainage area of 46784000. To be sure, it is the runoff of drainage basin 46784000 that supplies water to meet the demand for all the irrigated area in 46784000´.

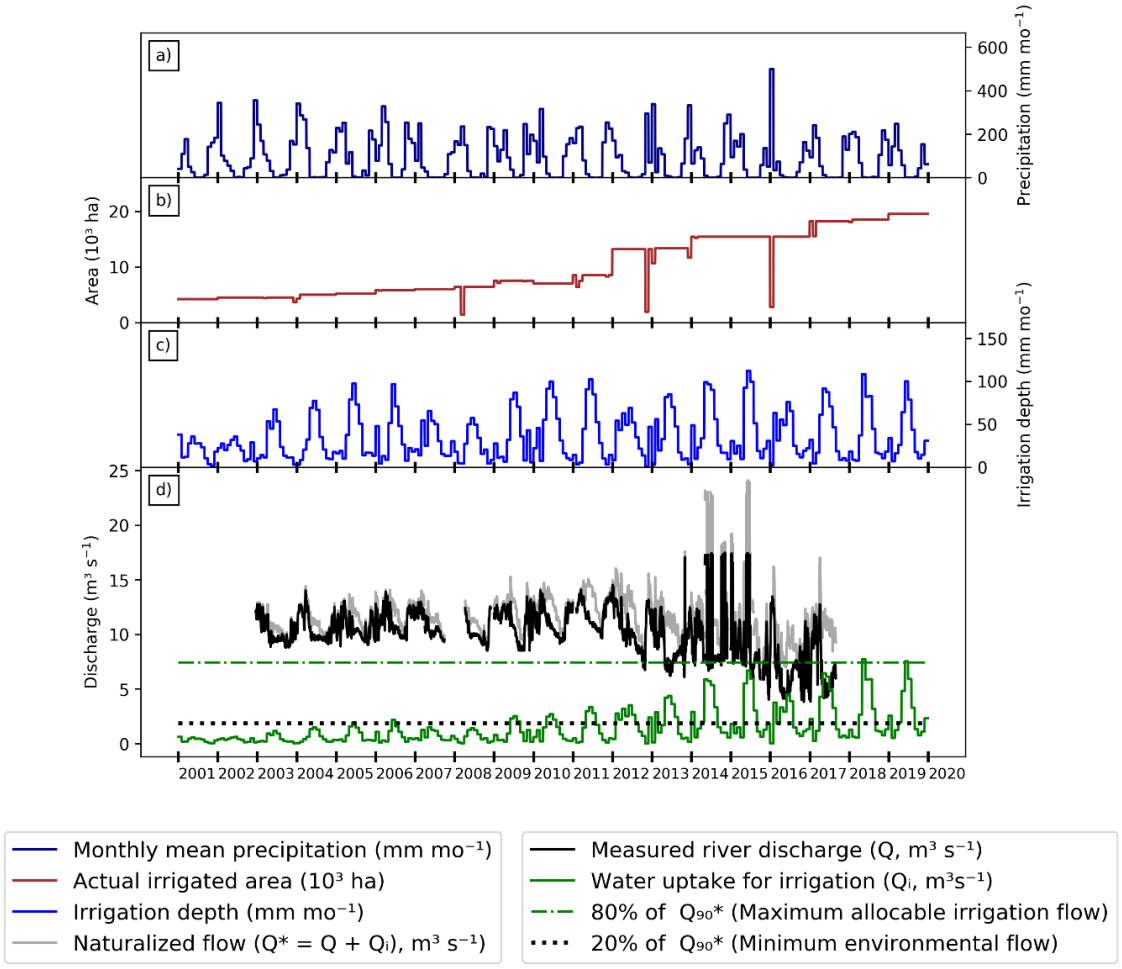

Figure 1. 7 Integrated results of flow station 46784000′ in the Grande basin: (a) monthly average precipitation series from 2001 to 2019; (b) actual irrigated area per month from 2001 to 2019; (c) monthly irrigation depth from 2001 to 2019; (d) measured (Q) and naturalized (Q*) river discharge and irrigation uptake (Q_i), where $Q^* = Q + Q_i$. The green and black dashed lines represent the minimum environmental flow and maximum allocable irrigation flow, respectively.

The increase of irrigated area is the main factor responsible for the change in Q_i over time (Figure 1.7d). After 2012, the peaks of Q_i increase quickly during the dry season, to the point that Q_i exceeds 80% of Q_{90}* in both May 2018 and June 2019. This rapid evolution also substantially affects the river flow (Figure 1.7d). The increase of Q_i occurring between 2012 and 2019 coincides with a rapid decline in the measured river flow. Similarly, to the Rio de

Janeiro, grants for surface water use represent 93% of the total grants in this region. Moreover, our attempt to naturalize the river flow has limitations for applications in such a small basin with high water use. Despite these limitations, there is no doubt that irrigation has been causing a significant impact in this sub-basin. Finally, similarly to the Rio de Janeiro, despite apparent overuse of surface water resources, minimum discharges are still much higher than the minimum environmental flow.

1.4 Discussion

This work is a first attempt to diagnose and monitor water used by irrigation and the resulting water stress in a region with intense irrigation growth—Western Bahia in Brazil. While actual Q_i measurements at pumping sites are not widely available, remote sensing provides the necessary data for an initial analysis. Here, I combined remote sensing data with discharge measurements to investigate the most concerning scenarios among the sub-basins, successfully providing an initial diagnostic tool for water use conflict and water insecurity situations. The results for the Corrente sub-basins show that there are no water conflicts or water insecurity situations in this basin. Two reasons may explain this comparatively comfortable scenario. First, compared with the Grande basin, the expansion of the irrigated area in the Corrente basin is more recent, according to the center pivot maps produced by (Pousa et al., 2019). Because of the notorious example of the water stress of its northern neighbor, the expansion of irrigation in the Corrente is happening under more careful governance. An example of this governance is the request by the Rio Corrente Basin Committee on 11 December 2015 to temporarily suspend the concession of water use permits in the basin until further criteria for water permits are defined (CBHRC, 2015). This request was presented to the environmental agency of the state of Bahia (INEMA—Instituto do Meio Ambiente e Recursos Hídricos), even though the water use for irrigation represents no more than 16.3% of the Q_{90}*

in the basin (Table 1.2). Second, the substantial number of center pivots already installed and the low Q_{imax}/Q_{90}* ratio both indicate that the farmers are managing planting dates to avoid using significant amounts of water during the low-season flows.

A different situation is found in the Grande sub-basins, which contains the three most critical cases analyzed. As detected in Pousa et al. (2019) and confirmed here, the irrigators of sub-basin 4657000 (Rio de Janeiro) have been working under water stress since the beginning of the millennium. However, I have only identified water use conflict situations in recent years. Water stress has also been a problem during this period in sub-basin 46784000 (Rio Branco), where I have identified water conflict situations since 2018. Although I do not see the same happening in the larger 46550000 sub-basin, the recent expansion of irrigated area and of the water amount used for irrigation indicates a tendency in the Grande basin.

In addition to the water resources diagnostic, our study also provides a first attempt to construct a data set for irrigation monitoring in Western Bahia. Here, I used three-day water balances to monitor the monthly amount used by irrigation. An analysis of the entire time series (Figures 1.4, 1.5, and 1.7) indicates consistent performance by our estimation method. The interview data collected by Pousa et al. (2019), which estimates a maximum irrigation depth ranging from 100 to 150 mm $month^{-1}$, is quite similar to our results. In addition, the months of high (April to June) and low (November to March) irrigation depth (Figures 1.4c, 1.5c, and 1.7c) match with the intervals between planting and harvest date practiced in the region (CONAB, 2023) and the irrigated area identified by our NDVI classification. Indeed, the MOD16A2 ET product has a strong correlation with vegetation greenness, as its algorithm depends on remote sensing data for leaf area index and fraction of absorbed photosynthetically active radiation (Biggs et al., 2016).

Although our data set does not have adequate temporal or spatial resolution for use in field irrigation management, it is useful for basin-scale analysis. An analysis of Figure 1.7

indicates that water use conflicts may arise quite soon in 46784000′ as the regional precipitation and river flow decrease (Pousa et al., 2019). It is important to note that the length of the river flow time series available for Rio Branco at Savana (2003–2017) is too short to account for a representative evaluation of the effects of the natural climate variability. However, there is no doubt that irrigation has been causing a significant impact in this small sub-basin.

The situation in sub-basin 46784000′ also portends similar potential problems in other sub-basins without discharge measurements. It is likely that other small rivers in Western Bahia are currently facing a similar water stress scenario or will be soon. The need for dense monitoring of the water resources in this region is well known, and there is a somewhat extensive network of federal, state, and even private river flow gauges that have been set up in the last decade or so, with a few installed as late as 2019. However, as with the 46784000 gauge, their time series are still too short for a representative hydroclimatic characterization of the sub-basins.

My results support the conclusions by Pousa et al. (2019) that there is an urgent need for hydroclimatic monitoring in Western Bahia. The setup of a "situation room," in which field measurements and remote sensing products like the one described here are collected and analyzed in near-real-time, would be a fundamental step toward better management of water resources in Western Bahia, in particular in the small basins.

In 2019, INEMA took a significant step toward the creation of a monitoring system with the publication of ordinance 19,452/2019, with norms for water measurement and reporting for monitoring purposes in the state. Although this ordinance has not yet produced practical results in terms of data flow, in the future, this in situ data set will complement the monitoring by remote sensing in several ways: first, the field data may be used for further calibration and validation of the remote sensing products; second, our remote sensing product may provide a baseline for spatial consistency of the regionally consolidated in situ data; third, the remote

sensing data provide a long-term time series that will be complemented by the field data; and finally, my remote sensing product may help to fill in gaps due to field measurement failures.

Another issue is the relatively high error in ET_a estimates at short time scales. In this work, I could reduce the bias of the remote sensing estimates by calibrating them against monthly ET field data. Still, two restrictions limited the performance of the adjusted model. The first is the coarse resolution of the MOD16 product (500 × 500 m, or 25 ha) compared to the typical size of a center pivot (100–150 ha), and the second is the lack of direct measurements of water application rates. My estimates can be improved in the future using remote sensing ET products based on higher-resolution data, such as from the Visible Infrared Imaging Radiometer Suite (VIIRS) sensor and the in-situ pumping data described above.

1.5 Conclusions

In this study, I use remote sensing products to assess the amount of water used for irrigation in Western Bahia, Brazil. The results demonstrate that the use of remote sensing products is a powerful tool to characterize the irrigation scenario in the region and its potential to identify critical water stress situations in small sub-basins. The amount of water used by irrigation combined with river gauge data can diagnose water use and water stress situations in areas with intense irrigation growth. The product developed here is a first contribution to provide stakeholders (government agencies, agribusiness, and organized civil society) with the necessary data to manage the water resources of the region.

Three sub-basins presented the most critical conditions for water conflicts: The Rio Grande upstream of the Barreiras station (46550000), the Rio de Janeiro upstream of the Ponte Serafim station (46570000), and the Rio Branco upstream of the Savana station (46784000). An in-depth analysis of these sub-basins shows that, despite the high water stress, water use for

irrigation has been steadily increasing, pushing the water use to its limits, particularly in Rio de Janeiro and Rio Branco.

Despite these promising initial results, I believe they can be improved in the near future. The emergence of new remote sensing evapotranspiration products at higher resolution, new sensors, and availability of new ground data will soon provide significant improvements to the monitoring of the water resources in this region.

Chapter 2: Enhancing Diagnosis of Water Use by Irrigation through Remote Sensing Products: A Case Study in Mato Grosso, Brazil.

Abstract

Irrigated agriculture has experienced growth in recent decades, contributing significantly to global food production. However, the activity faces challenges due to the effects of climate change. The irregularity of rainfall affects the quantity of water resources, such as river flow and aquifers, reducing the availability of water for irrigation practices. Establishing a monitoring system for irrigation becomes crucial for sustainable use, avoiding the emergence of conflicts among water users in regions intensively occupied by the activity. As a viable and cost-effective alternative, the remote sensing products of evapotranspiration are potential tools to measure the irrigation demand for water. In this study, I improved existing methods by leveraging a new dataset from the Global Daily Evapotranspiration (GLODET) project to enhance water usage estimates in a region intensely irrigated located in Mato Grosso, the main grain producer state of Brazil. To assess the effectiveness of the new remote sensing products against evapotranspiration products from MODIS data (MOD16A2GF product), I employed data from an eddy covariance tower located close to the region. In general, the results indicate that the new GLODET data (RMSE = 2.19, MAE = 1.58, r = 0.31) align more closely with flux tower measurements compared to the MODIS data (RMSE = 2.53, MAE = 2.29, r = 0.69), which consistently underestimates evapotranspiration across different seasons. I also apply both products to produce a temporal series from 2001 to 2022 of monthly irrigation demand for the region. The method consists of a 4-day water balance, integrating both evapotranspiration datasets and precipitation data obtained from CHIRPS (Climate Hazards Group Infrared Precipitation with Stations). The time series of water uptake for irrigation obtained here illustrates the pattern of water use in the region, with peaks in dry months and lows in rainy months. The combination of these results with river gauge information in future analyses could

provide valuable insights into the water resource studies, identifying potential conflict areas, and regions suitable for irrigation expansion.

2.1 Introduction

Irrigation has become a growing agricultural activity, expanding in both size and significance worldwide. This activity plays a vital role in global food production, contributing to increased yields and improved crop quality. Irrigation, as a solution, could also offer support and resilience for crops to navigate potential drought periods (Rosa, 2022). Nevertheless, the dependence of river flow and aquifer recharge on rainfall (Cambraia Neto et al., 2021; Luiz Silva et al., 2019; Marques et al., 2020; Salmona et al., 2023), also renders irrigation susceptible to climate change. Therefore, implementing a monitoring system is an essential step to support the sustainable expansion of irrigation. By providing valuable information on irrigation water consumption, the system becomes a crucial tool for facilitating informed decision-making on when, where, and how much irrigation is viable (Pousa et al., 2019; Santos et al., 2020).

Monitoring water consumption in irrigation involves measuring plant evapotranspiration (ET). Remote sensing allows for the indirect measurement of evapotranspiration by capturing data from a distance using satellite sensors (Zhang et al., 2016). Furthermore, considering that this method provides a cost-effective alternative to on-site measurements, using remote sensing products makes it the optimal choice as a component of comprehensive irrigation monitoring and management (Bispo et al., 2022; Brocca et al., 2018; Gonçalves et al., 2022; Jalilvand et al., 2019).

Various algorithms have been employed with remote sensing data over the years to estimate energy fluxes and quantify evapotranspiration (ET) (Allen et al., 2007; Anderson et al., 1997; Bastiaanssen et al., 1998; Kustas, 1990; Roerink et al., 2000; Su, 2002). In Santos et al. (2020), the MOD16A2 product of the MODIS Global Evapotranspiration Project was

utilized to generate a temporal series of applied irrigation depth in highly irrigated basins located in Western Bahia. The methodology obtained positive results and effectively captured the general pattern of irrigation in the basins, providing valuable insights into the irrigation situation when compared with river data. However, the authors argued that employing higher-resolution remote sensing data could address potential limitations associated with the product used.

For this work, I essentially applied the Santos et al. (2020) method to estimate the water used by irrigation in a high irrigate zone in Mato Grosso, which is the largest grain-producer state in Brazil. In 2022/2023, Mato Grosso contributed significantly to national grain production, with 100.9 million tons, accounting for 31% of the total grain production in the country (CONAB, 2023). Besides, with its well-established agricultural area and favorable terrain and climate conditions, the state demonstrates the most significant potential for the expansion of irrigation in Brazil (ANA, 2021). A study conducted in partnership between the National Water Agency and FAO reveals that the state has approximately 10.4 Mha of previously occupied areas are available for expansion of irrigation (Rocha Júnior, 2020).

I enhanced the Santos et al. (2020) approach by using a new ET dataset provided by the Global Daily Evapo-Transpiration (GLODET) project. In contrast to MODIS, which offers an 8-day composite with a pixel resolution of 500 m, the new ET data provides daily spatial information with a higher resolution of 375 m per pixel. The GLODET platform, hosted by the University of Nebraska-Lincoln, utilizes the ALEXI approach model, developed by the USDA (United States Department of Agriculture) in conjunction with Visible Infrared Imaging Radiometer Suite (VIIRS) imagery, to estimate ET for all vegetated areas worldwide. The integration of an advanced algorithm and VIIRS data allows for a more accurate assessment, providing ET data with improved time and pixel resolution.

Therefore, this work is divided into two parts. First, the ET data from the two datasets (MOD16 and GLODET) are compared with measured data obtained from an eddy covariance tower to analyze the accuracy and reliability of the remote sensing datasets. The comparison aims to assess how the satellite-derived ET data aligns with ground-based measurements. In the second part, both datasets are used to quantify irrigation. This involves applying the Santos et al. (2020) method and integrating the enhanced dataset. The goal is to refine and improve water usage estimates, providing new insights into the use of remote sensing products in irrigation monitoring.

2.2 Material and Methods

2.2.1 Study area

The Rio das Mortes Irrigation Zone (RM) is situated in southeastern Mato Grosso, located within the Cerrado biome, and around 76% of its territory is already occupied by agriculture (MAPBIOMAS, 2023). According to Köppen's climate classification (Peel et al., 2007), the RM experiences a predominantly Aw (tropical Savanna) climate, characterized by distinct dry and wet seasons: a rainy season extending from October to April, and a dry season prevailing from May to September. According to data from ANA (the National Water Agency of Brazil), in the period between 2000 and 2017, the area covered by center pivots grew by 790%, increasing from 32 pivots in 2000 to 253 in 2017. In RM, the predominant use of center pivot systems is for seasonal crops, including soybeans, corn, and cotton. These crops can have two or more rotations per year, underscoring the intensive agricultural practices in the area.

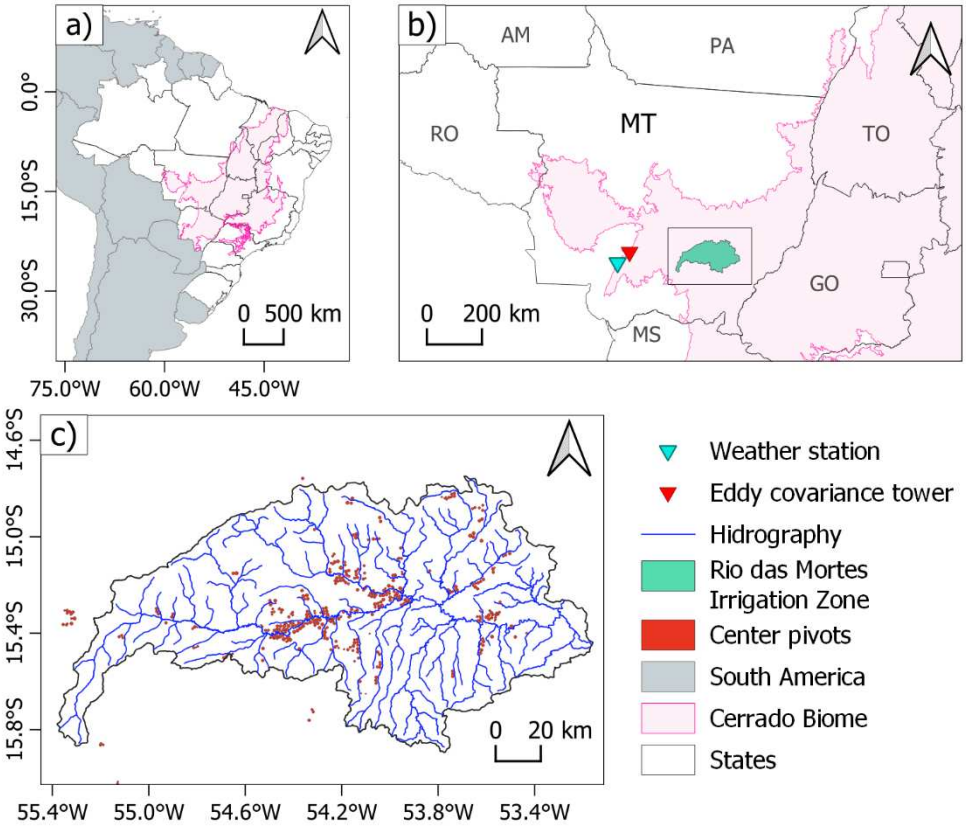

Figure 2. 1 (a) Cerrado biome extension. (b) Rio das Mortes Irrigation zone (RM), eddy covariance tower and weather station location. The red triangle marks the eddy covariance, and the blue one indicates the weather station location. MT is the Mato Grosso state. AM, PA, TO, RO, GO, and MS are the states of Amazonas, Pará, Tocantins, Roraima, Goiás and Mato Grosso do Sul, respectively. (c) Center pivot location and hydrography. The center pivots map was obtained from ANA (2021) and it refers to the year of 2017.

2.2.2 Remote Sensing Data

This study analyzed two remote sensing products of ET to obtain the water use diagnostics in RM. The first product is the MOD16A2GF Version 6.1 Evapotranspiration/Latent Heat Flux (ET/LE) product. The MOD16A2GF is an 8-day composite dataset, gap-filled at year-end, and produced at 500 m pixel resolution. Derived from the Moderate Resolution Imaging Spectro-radiometer (MODIS) sensor on the Terra satellite,

the MOD16A2GF dataset is estimated using Mu et al. (2011) improved ET model (MOD16) over previous version elaborated by Mu et al. (2007). The algorithm logic is based on the Penman–Monteith equation (PM), where estimates latent heat flux (LE) and/or sensible heat flux (H) directly in conjunction with the energy balance equation. The pixel product represents the sum of evaporation from the dry canopy (transpiration), wet canopy evaporation (rainfall interception), and soil (Mu et al., 2007, 2011).

The MOD16 model also has two components that calculate night and day separately, and two types of input data are used to estimate ET. The first one is derived from the Global Modeling and Assimilation Office (GMAO/MERRA), providing daily meteorological reanalysis, including solar radiation, air temperature, air pressure, humidity, current night vapor pressure, night air temperature, and incident shortwave radiation. The second input comprises products obtained through remote sensing from MODIS products, encompassing surface albedo for the calculation of net radiation (R_n), the fraction of photosynthetically active radiation (FPAR) for the R_n portioning between H and LE; the Leaf Area Index (LAI) to calculate the canopy resistances, and land cover data to allocate Phyto-physiological parameters included in the model.

Moreover, the 6.1 version of the MOD16 ET product presents several improvements over the previous version (6.0) by incorporating calibration changes (NASA, 2023). The gap-filled MOD16A2GF has also addressed poor-quality inputs from the 8-day Leaf Area Index/Fraction of Photosynthetically Active Radiation (LAI/FPAR) dataset using Quality Control (QC) labels for each pixel (NASA, 2023). In cases where an LAI/FPAR pixel did not meet the quality screening criteria, its value is determined through linear interpolation (NASA, 2023).

In addition to the MOD16A2GF product, this study also utilized the Global Daily Evapo-Transpiration (GLODET) project database. GLODET is a free platform for visualizing

and downloading a spatial dataset of ET (https://glodet.nebraska.edu/#/), hosted by the Daugherty Water for Food Global Institute (DWFI) at the University of Nebraska. The GLODET database comprises daily maps with a spatial resolution of 375 m. For this study, only the grid covering Brazil's southern and central regions, below the latitude 15° S, was utilized.

The data are computed using the two-source energy balance model ALEXI (Atmosphere-Land Exchange Inverse), developed by the Agricultural Research Service of the U.S. Department of Agriculture (GLODET, 2023). The ALEXI model employs a dual-source approach, conceptualizing the Earth's surface as a combination of distinct soil and vegetation elements. This methodology involves the separate computation of LE for both the canopy and soil components (Anderson et al., 2007a, 2007b).

To estimate ET, the ALEXI algorithm utilizes the morning surface temperature. To account for diurnal temperature variations, the two-source model is coupled with an Atmospheric Boundary Layer (ABL) model, capturing temperature changes throughout the day by considering the boundary layer's dynamic movement. Thus, the model is applied at two instances during the growth phase of the boundary layer height: T_1 = 1.5 h and T_2 = 5.5 h (after local sunrise). In the GLODET database, a regression model trained with GOES data utilizes temperature differences from the Visible Infrared Imaging Radiometer Suite (VIIRS) to predict morning temperature changes (Anderson et al., 2007a; Hain & Anderson, 2017). In addition, ALEXI integrates various levels of information from the land surface and atmosphere. The inputs include: 1) LAI and vegetation cover fraction, 2) land surface albedo, 3) incoming solar radiation, 4) surface meteorological data, 5) morning temperature profile, 6) land cover and vegetation type, and 7) cloud mask (GLODET, 2023).

I used data ranging from 2001 to 2022 for the MODIS product, and data ranging from 2013 to 2022 for the GLODET dataset. Additionally, to address any gaps within the GLODET data, I applied the linear interpolation technique to fill the missing days.

I also utilized daily precipitation data from CHIRPS (Climate Hazards Group Infrared Precipitation with Stations, https://www.chc.ucsb.edu/data/chirps) to estimate water uptake for irrigation. CHIRPS is a high-resolution precipitation dataset that integrates infrared satellite imagery and ground station data to estimate global rainfall patterns (Funk et al., 2015). This product has a spatial resolution of 0.05°, providing quasi-global coverage, and is available from 1981 to the present.

2.2.3 ET field measurements

One representative site near RM was employed to validate the ET remote sensing products. The site is an eddy covariance tower (EC) situated in the Cerrado biome at Fazenda Arco-Iris in the southern of Mato Grosso state (15°10′38.88″S, 56°58′3.41″W) (Figure 2.1). The data was collected and analyzed for the first time by Biudes et al. (2022).

According to Biudes et al. (2022), the sensors used include an NRLITE (Kipp & Zonen, Delft, The Netherlands) to measure R_n, HMP-45AC (Vaisala Inc., Woburn, MA, USA) to measure T_{air}/RH and an HFP01 (Hukseflux BV, Delft, The Netherlands) to measure G as well as a CR1000 datalogger (Campbell Scientific, Inc., Logan, UT, USA) to read and store the data at 10 Hz. The raw data from the EC system were processed using EddyPro Advanced software (LICOR, 2023) and REddyProc tool (Wutzler et al., 2018) was used for data gap filling. Field measurements from EC were acquired from 2021 to the beginning of 2023, and have a time resolution of 30-min.

An eddy covariance flux tower is used in the field to directly measure the energy balance components for estimating evapotranspiration. However, if these field measurements of surface fluxes are not consistent with the energy balance equation ($R_n = H + LE + G$), some

adjustments are needed to assure the energy conservation, decreasing the energy discrepancy (H + LE) / (R_n – G). In this study, I used the Bowen Ratio procedure suggested by Twine et al. (2000) to adjust the eddy covariance data by forcing the closure of energy balance. In this method, the LE is added by a factor (LE + Δ) estimated by Equation 2.1:

$$\Delta = \frac{(R_n - G) - \left(1 + \frac{H}{LE}\right) \cdot LE}{1 + \frac{H}{LE}} \quad (2.1)$$

where R_n is the net radiation (W m^{-2}), G is the soil heat flux (W m^{-2}), H is the sensible heat (W m^{-2}) and LE is the latent heat (W m^{-2}). The closure procedure was applied for each 30-minute interval of eddy covariance data. Then, the 30-minute latent heat flux corrected by Δ (LE + Δ) was convert to ET by using the latent heat of evaporation (λ):

$$ET = \frac{LE + \Delta}{\lambda} \quad (2.2)$$

where λ = 2264.705 kJ kg^{-1} was adopted. Thus, the daily measured ET ($ET_{MEASURED}$) was obtained by accumulated the 30-min ET, excluding values during nighttime periods (when R_n < 0). A weather station near the eddy covariance tower site was also used to verify the ET measured from EC. The climate variables provided were used as input in the Penman-Monteith model to estimate the reference ET (ET_{ref}). The weather station is also located in Mato Grosso state, about 60 km away from the EC site (16°29′53.52″S, 56°24′46.23″W).

The accuracy of the ET_{MODIS} and ET_{ALEXIS} products was assessed using the mean absolute error (MAE, Equation 2.3) and root mean square error (RMSE, Equation 2.4).

$$MAE = \sum \frac{|E_t - O_t|}{n} \quad (2.3)$$

$$RMSE = \sqrt{\sum \frac{|E_t - O_t|^2}{n}} \quad (2.4)$$

where E_t is the estimated value for the time t, O_t is the observed, and n is the number of observations. The MAE indicates the average absolute deviation distance, representing the average magnitude of the errors. On the other hand, the RMSE measures the dispersion of estimated values from the actual measurements. An RMSE value of 0 signifies a flawless agreement, reflecting a perfect match between the model's predictions and the measured data.

2.2.4 Estimating of irrigation depth and actual irrigated area

In this study, I estimated irrigation depth, water uptake for irrigation, and actual irrigated area using both ET products for RM region. To estimate these variables, we followed the methodology developed by Santos et al. (2020), briefly described below.

The first step of computing the irrigation situation in the irrigation zone is the center pivot mapping. To generate these maps, I implemented four key steps, as proposed by Santos et al. (2020) and Pousa et al. (2019): (i) processing imagery from Landsat 5, 7, and 8 using the Google Earth Engine cloud to mosaic the images for the region and filter the pixels first for the dry period (April to September) and later for the NDVI median of the study region; (ii) merging the filtered map with other center pivot maps to produce an initial map for the region; (iii) removing duplicated features and topology errors; and (iv) validating positional accuracy through a trend and precision analysis to produce a final map without trends in center pivot sizes and locations with accuracy adequate to the scale of 1:150,000 that is compatible with the resolution of the Landsat images (30 m). However, this dataset should be considered a data set of available infrastructure for irrigation, as it does not inform when there is a crop on the field that is being irrigated.

To estimate ET for each center pivot, we aggregated all MODIS ET and ALEXI ET pixels within the pivot area. This involved calculating a pivot average, considering the

proportion of area covered by each pixel within the pivot. I applied a modified version of the methodology developed by Santos et al. (2020) using a four-day time step. This four-day period corresponds to half the time interval of the 8-day MODIS product. In addition, I did not implement the ET correction proposed by Santos et al. (2020) in this study due to the absence of cropland ET ground data for validation. The irrigation depth (D) was calculated according to Equation 2.5:

$$D(i) = \max\left(\frac{ET(i) - P(i)}{\varepsilon}, 0\right) \tag{2.5}$$

where P(i) is the four-day CHIRPS precipitation on pivot I, ET(i) is its four-day ET estimated using ET products from MOD16 model (ET_{MODIS}) and ALEXI model (ET_{ALEXI}), and ε represents the media efficiency of a center pivot, set at 0.85 as adopted by Santos et al. (2020). When P(i) > ET(i), the crop ET demand was fully satisfied by the precipitation, and there was no irrigation in the center pivot in that period, so D(i) = 0. Next, I accumulated the computed four-day water application rate monthly. Thus, this will result in two monthly databases of irrigation depth, one calculated using ET_{MODIS} (D_{MODIS}) and another using ET_{ALEXI} (D_{ALEXI}). The water uptake for irrigation from each center pivot is simply the product of the water application rate, denoted as D(i), measured mm month^{-1}, multiplied by the area of the center pivot in hectares, with units adjusted to m³ s^{-1}. This approach yields two datasets representing water used for irrigation, one based on the depth calculated by D_{MODIS} (Q_{MODIS}) and the other by D_{ALEXI} (Q_{ALEXI}).

2.3 Results

2.3.1 Eddy covariance energy balance closure

The closure procedure aims to maintain energy conservation by aligning the energy fluxes, reducing discrepancies in the relationship between the amount of available energy (Rn - G) and the partitioning of latent and sensitive heat flux (LE + H). Figure 2.2 illustrates the results of the energy closure performed with the EC data. Figure 2.2a presents the conditions before the closure procedure, while Figure 2.2b presents the conditions after. Following the closure, there was an enhancement in the correspondence between values, marked by an increase in the linear correlation among the points (from r = 0.91 to r = 0.95). Some outliers were observed after the closure process; however, their ET values were assimilated into the daily ET accumulation.

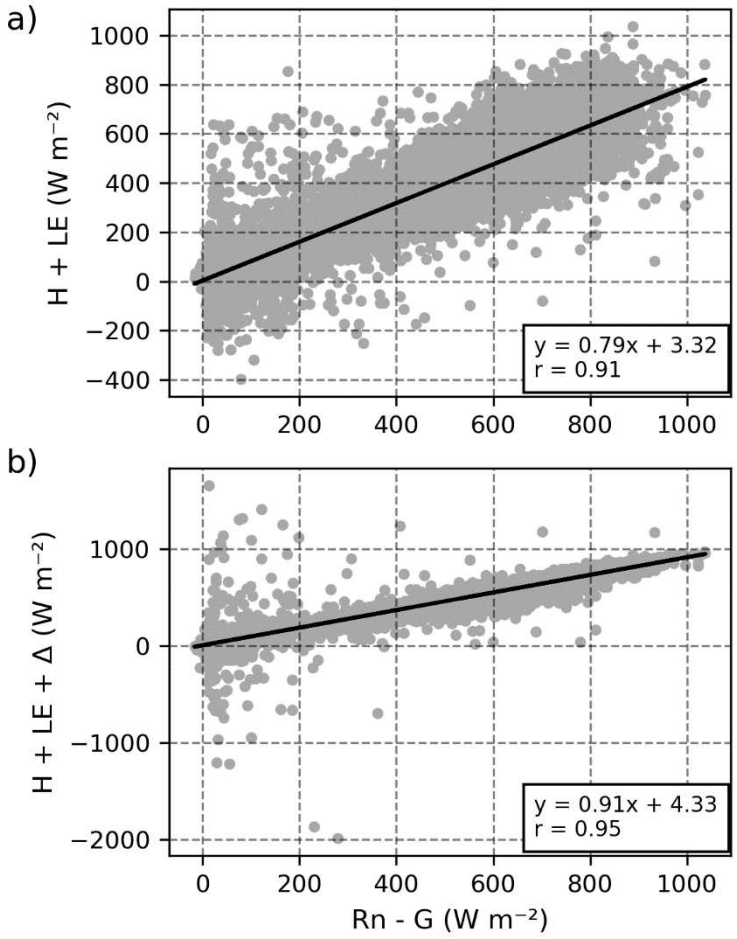

Figure 2. 2 Comparison between turbulent and non-turbulent terms. (a) 30-min. raw data (b) 30-min adjusted data (LE + Δ). The raw data represents all data collected by EC except the moments when Rn < 0.

The daily $ET_{MEASURED}$ was computed using the closure procedure (Equation 2.1) and compared to the daily reference evapotranspiration (ET_{ref}). In Figure 2.3a, the daily precipitation provided by CHIRPS dataset at the weather station site is illustrated, providing context for the meteorological conditions. Figure 2.3b delineates the dynamic patterns of $ET_{MEASURED}$ and ET_{ref}. Both ET patterns are similar, with ET_{ref} increasing slightly earlier than $ET_{MEASURED}$. Additionally, values of ET_{ref} and $ET_{MEASURED}$ become similar during the rainy months (from October to March), demonstrating a consistent pattern in $ET_{MEASURED}$. During

the dry season (from April to September), the ET_{ref} is higher than $ET_{MEASURED}$ due to the Penman-Monteith method not incorporating water restrictions into its calculation.

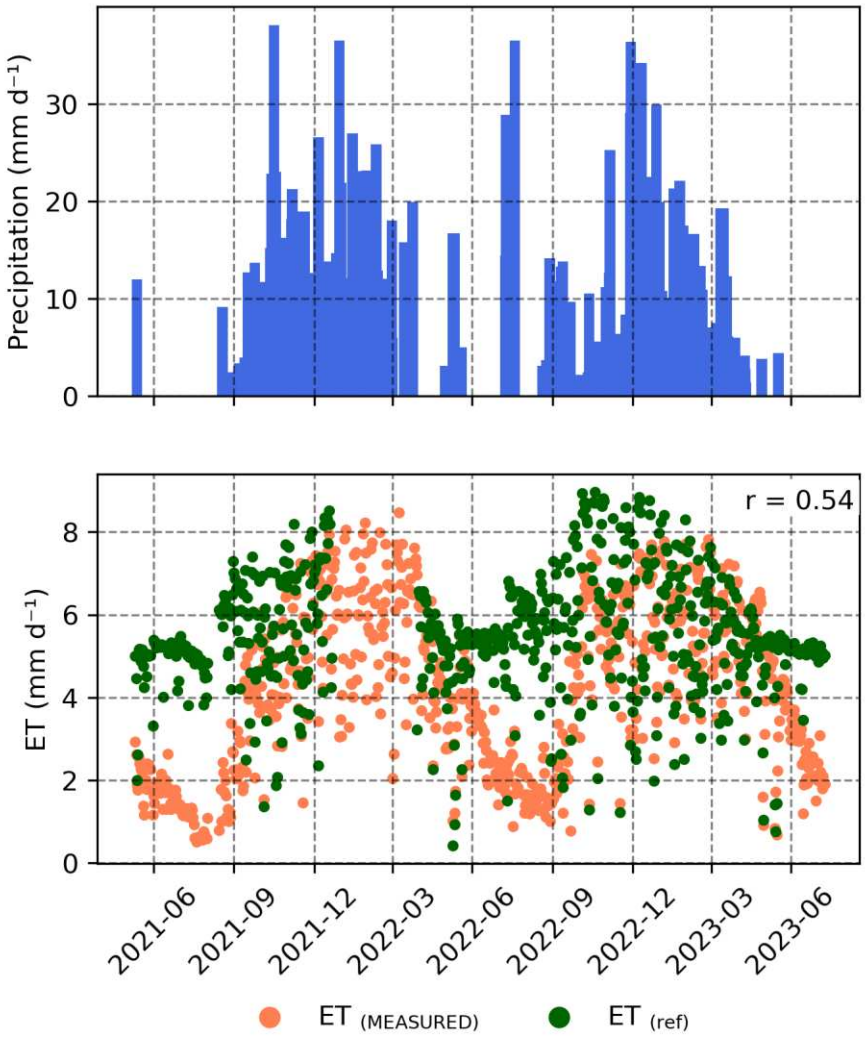

Figure 2. 3 (a) Daily precipitation in the weather station site (data obtained from CHIRPS dataset). (b) Correlation between $ET_{MEASURED}$ and ET_{ref} is 0.54.

2.3.2 Comparison of $ET_{MEASURED}$ and ET_{MODIS}/ET_{ALEXIS}

Figure 2.4 illustrates the comparison results between $ET_{MEASURED}$ and two distinct datasets: ET_{MODIS} (Figure 2.4a) and ET_{ALEXI} (Figure 2.4b). To align with the 8-day temporal resolution of the ET_{MODIS} dataset, I aggregated the $ET_{MEASURED}$ values over 8-day intervals, resulting in a dataset with 37 points. In contrast, the ET_{ALEXI} dataset provides daily data, contributing to a more extensive dataset with 359 points. The comparison reveals that the

ET_{MODIS} model consistently underestimates evapotranspiration, as indicated by all data points falling below the 1:1 line (Figure 2.4a). Conversely, the ET_{ALEXI} results demonstrate a more balanced distribution around the 1:1 line than ET_{MODIS}.

Moreover, the ET_{MODIS} dataset demonstrates a correlation coefficient of r = 0.69 with $ET_{MEASURED}$, as outlined in Table 2.1. The corresponding MAE and RMSE for ET_{MODIS} are 2.29 mm day^{-1} and 2.53 mm day^{-1}, respectively. On the other hand, the results for ET_{ALEXI} show a correlation coefficient of r = 0.31, while the MAE and RMSE values are 1.58 mm day^{-1} and 2.19 mm day^{-1}, respectively.

Table 2. 1 Statistical metrics of the remote sensing ET products (ET_{MODIS} and ET_{ALEXIS})

ET estimates	r	MAE (mm dia^{-1})	RMSE (mm dia^{-1})
ET_{MODIS}	0.69	2.29	2.53
ET_{ALEXI}	0.31	1.58	2.19

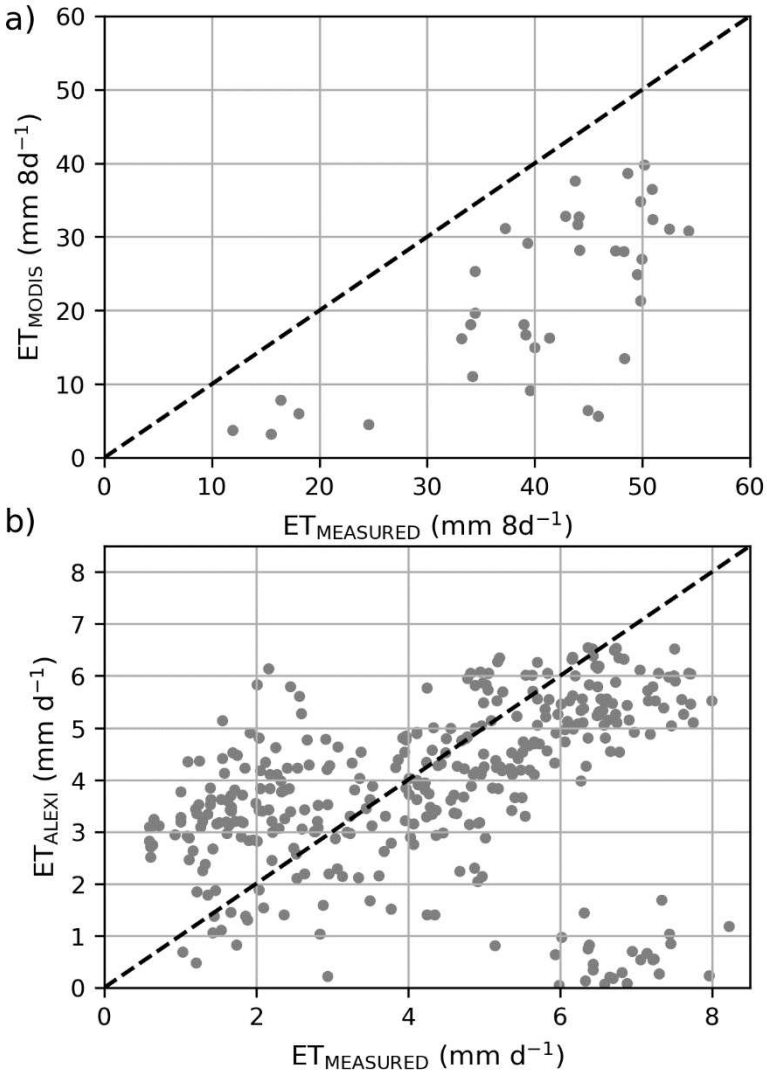

Figure 2. 4 (a) Scatterplot of Eddy covariance data ($ET_{MEASURED}$, mm 8 day^{-1}) and estimated (ET_{MODIS}, mm 8 day^{-1}). (b) Scatterplot of Eddy covariance data ($ET_{MEASURED}$, mm day^{-1}) and estimated (ET_{ALEXI}, mm day^{-1}). The dashed lines represent the 1:1 line.

2.3.3 Application: irrigation diagnostic of Rio das Mortes irrigation zone

Figure 2.5 illustrates the irrigation diagnostic for the Rio das Mortes irrigation zone. The totals are for center pivots only, weighted by each pivot´s area. The observed monthly precipitation pattern is indicative of the regional climate, characterized by two distinct seasons: the rainy season (October to April) and the dry season (May to September; Figure 2.5a).

Monthly precipitation exhibits significant variability, ranging from 0 to approximately 450 mm per month.

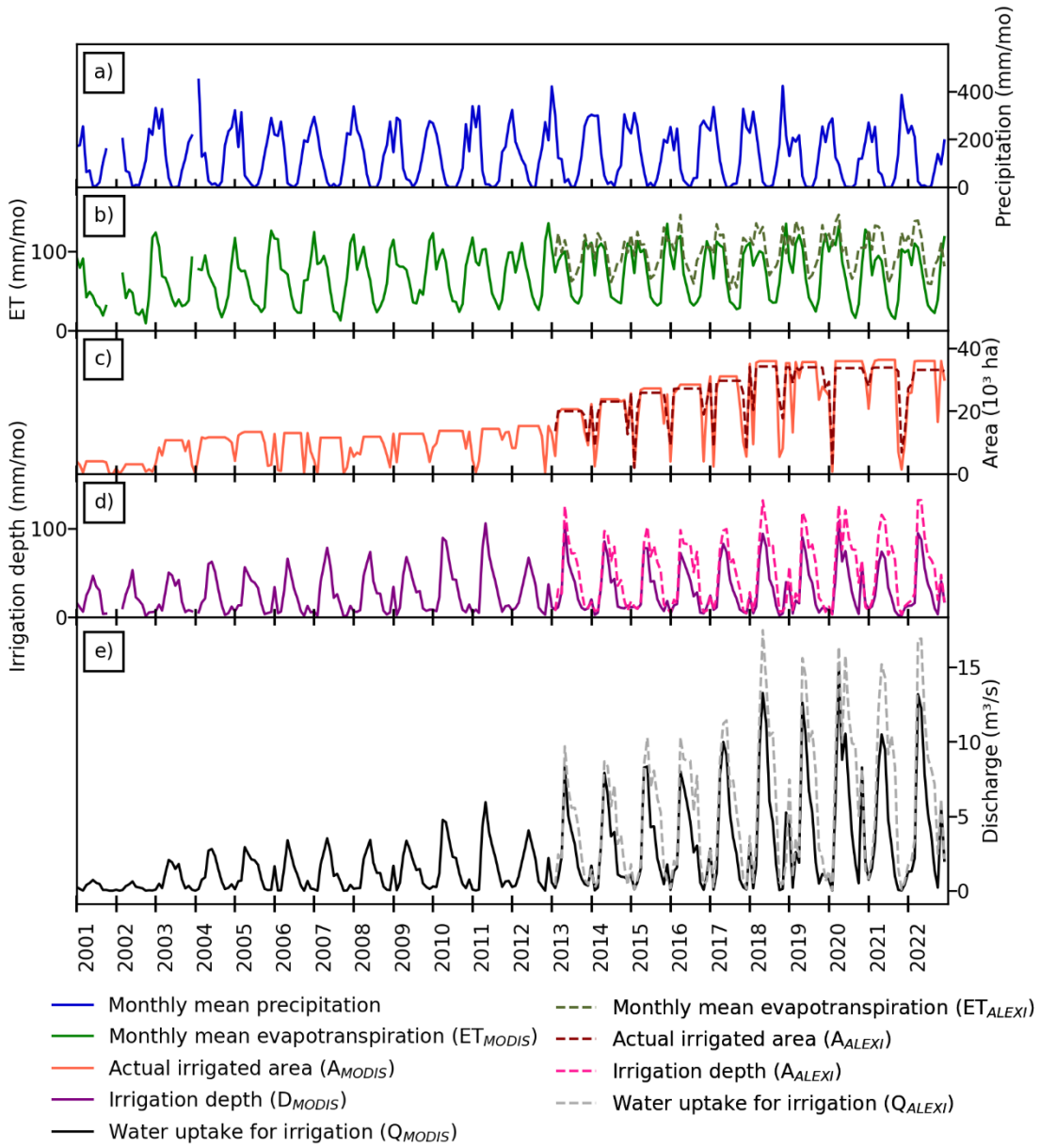

Figure 2. 5 Irrigation diagnostic for Rio das Mortes Irrigation Zone. (a) monthly average precipitation series from 2001 to 2022; (b) monthly average evapotranspiration (ET) series from 2001 to 2022; (c) actual irrigated area per month from 2001 to 2022; (d) monthly irrigation depth from 2001 to 2022; (e) water uptake for irrigation in $m^3 s^{-1}$ from 2001 to 2022. The dashed lines represent variables derived from ALEXI data, and the solid lines represent the variables derived from MODIS.

Evapotranspiration also shows significant seasonal variability for ALEXI and MODIS products, representing the dynamics of irrigated crops throughout the year. For the monthly ET derived from MODIS (ET_{MODIS}), the ET ranges from around 10 mm $month^{-1}$ in the dry season to approximately 135 mm $month^{-1}$ in the wet season. ET from the ALEXI product consistently demonstrates higher values than the MODIS product. During the dry season, ALEXI's ET ranges from approximately 50 mm to 150 mm per month during the wet season (Figure 2.5b).

Figure 2.5c illustrates the estimated irrigated area using ET products, $A_{ALEXI,}$ and A_{MODIS} (ha $month^{-1}$). In general, the calculated areas using MODIS and ALEXI products show a close resemblance. Both products exhibit a consistent pattern, demonstrating an increase in irrigated area from approximately 4,000 hectares in the dry season of 2001 to around 36,000 hectares in the dry season of 2022. As observed by Santos et al. (2020), the stability of the irrigated area over the months indicates that the irrigation systems operate throughout the entire year, with irrigation system operating less frequently in rainy months.

The average irrigation depth derived from both products (D_{ALEXI} and D_{MODIS}, mm $month^{-1}$) exhibits significant seasonal variability. Given that ET_{ALEXI} consistently surpasses ET_{MODIS}, D_{ALEXI} is also greater than D_{MODIS}. D_{ALEXI} ranges from less than 10 mm $month^{-1}$ in the rainy season to approximately 120 mm $month^{-1}$ in the dry season, while D_{MODIS} ranges from less than 10 mm $month^{-1}$ in the rainy season to around 100 mm $month^{-1}$ in the dry season (Figure 2.5d).

Figure 2.5e displays the results for water uptake for irrigation estimated using both products, Q_{ALEXI} ($m^3\ s^{-1}$) and Q_{MODIS} ($m^3\ s^{-1}$). Similar to the patterns observed for ET and D, Q_{ALEXI} is significantly larger than Q_{MODIS}. The values for Q_{ALEXI} range from around 1 $m^3\ s^{-1}$ in rainy season to 17 $m^3\ s^{-1}$, while for Q_{MODIS}, they range from 0 to 15 $m^3\ s^{-1}$.

Figure 2.6 shows the results for the comparisons between variables derived from the ALEXI ET product (A_{ALEXI}, ET_{ALEXI}, D_{ALEXI}, Q_{ALEXI}) and variables derived from the MODIS

ET product (A_{MODIS}, ET_{MODIS}, D_{MODIS}, Q_{MODIS}). The ALEXI-derived variables are typically higher than the MODIS ones, likely because of the higher resolution of the VIIRS imagery (375 m) compared to the MODIS imagery (500 m). All variables present a good correlation, with values of 0.97, 0.93, 0.92 and 0.92 for actual irrigated area, ET, irrigation depth and water uptake for irrigation, respectively.

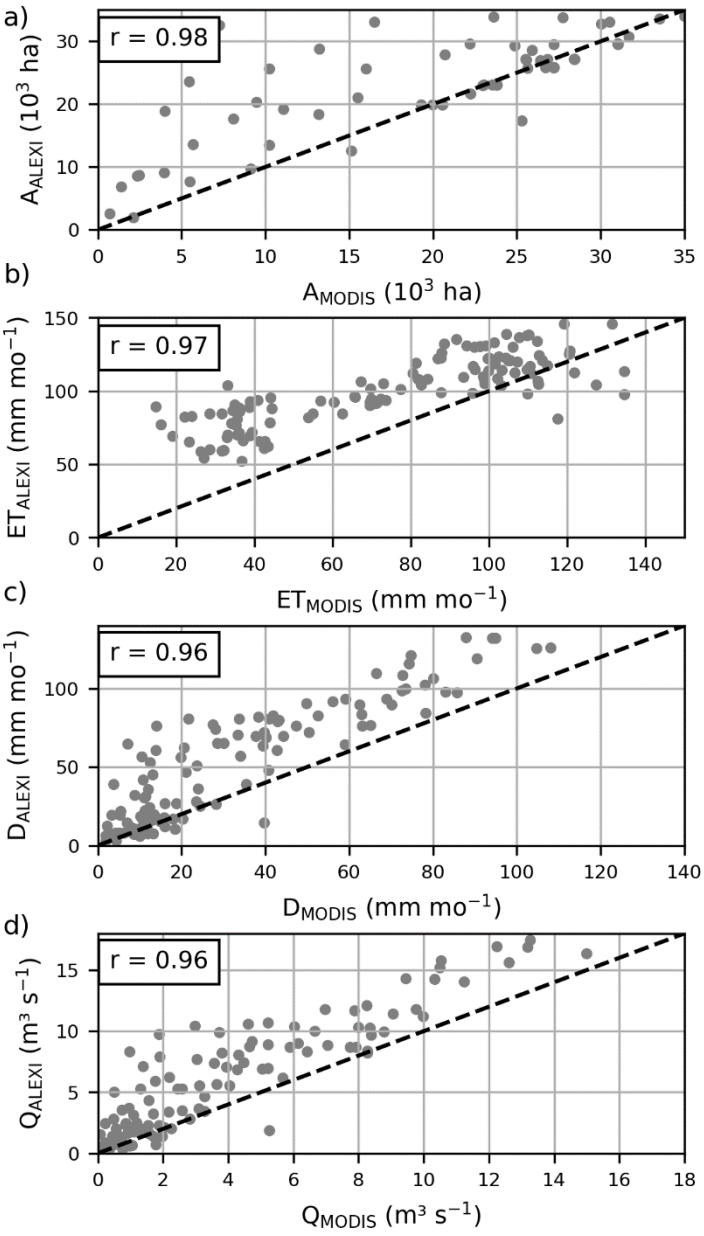

Figure 2. 6 Comparison between the variables (a) actual irrigated area, A_{ALEXI} and A_{MODIS}; (b) monthly evapotranspiration ET_{ALEXI} and ET_{MODIS}; (c) irrigation depth D_{ALEXI} and D_{MODIS}; (d) water uptake for irrigation Q_{ALEXI} and Q_{MODIS}. The dashed lines represent the 1:1 line.

2.4 Discussion

Over the years, numerous studies have already investigated the performance of various ET remote sensing products worldwide, employing MOD16 model (Aguilar et al., 2018; Biudes

et al., 2022; Cheng et al., 2020; Ramoelo et al., 2014; Salazar-Martínez et al., 2022; Souza et al., 2019), or ALEXI model (Anderson et al., 2007a; Salazar-Martínez et al., 2022). The identified differences between these methods in ET estimation can be attributed to a range of factors linked to the models, including parameters, physical processes, and input data. In addition, the environmental conditions and diverse landscapes may also affect the evaluation of the performance of remote sensing products.

The analysis of the correlation factors indicates a relatively better agreement between $ET_{MEASURED}$ and ET_{MODIS} ($r = 0.69$, Table 2.1) than between $ET_{MEASURED}$ and ET_{ALEXI} ($r = 0.31$, Table 2.1). However, the estimated ET_{MODIS} consistently showed underestimated values relative to the measurements obtained from the eddy covariance tower (Figure 2.4a). Previous validations of the MOD16 model have consistently demonstrated a tendency to underestimate ET in sparsely vegetated areas, including savanna (Mu et al., 2007; Ramoelo et al., 2014). This situation likely arises from a strong dependence of ecosystems in arid and semi-arid zones on soil moisture, a critical factor not directly incorporated into the algorithm (Brust et al., 2021). Instead, the model constrains soil evaporation and transpiration based on daily Vapor Pressure Deficit (VPD), relative humidity, and minimum air temperature (Mu et al., 2007; Mu et al., 2011).

The absence of explicit soil moisture information overlooks a fundamental control factor in the water balance affecting ET, leading to potentially significant errors (Brust et al., 2021; Michel et al., 2016; Miralles et al., 2016). Additionally, specific constraints adopted by the MOD16 algorithm to simulate vegetation behavior may further contribute to the observed underestimation. In Biudes et al. (2020), similar underestimations of ET were reported in the Cerrado using the same eddy covariance data for validation.

ET_{ALEXI} exhibited lower values of RMSE (2.19, Table 1) and MAE (1.58, Table 1) compared to ET_{MODIS} (RMSE = 2.53, MAE = 2.29, Table 1). Besides, as depicted in Figure 4b,

the data points exhibited a more favorable distribution around the 1:1 line than ET_{MODIS}. This indicates a more precise alignment of predicted values with $ET_{MEASURED}$, suggesting that ET_{ALEXI} demonstrates a closer agreement with the reference data. However, the widely dispersed behavior of the data points, indicated by a low correlation, suggests potential challenges in accurately quantifying fluxes within the model across different seasons.

These challenges likely arise from the persistent issue of addressing cloud-contaminated data in thermal-based approaches (Salazar-Martínez et al., 2022). ALEXI model, in particular, necessitates clear-sky conditions between time intervals t1 to t2 to obtain the requisite surface temperature data to simulate the linear rise of sensible heat during the morning boundary layer growth phase (Anderson et al., 2007a). The gap-filling procedure in the ALEXI model, as described by Anderson et al. (2007a) and implemented in the GLODET platform, may contribute to this issue. Anderson et al. (2007a) highlighted that the uncertainty in gap-filled ALEXI ET estimates can be twice as large as the ET generated by the algorithm under clear sky conditions.

The second part of this study involves the case study of RM region in which both ALEXI and MOD16 products were employed to diagnose irrigation in RM. The methodology followed the approach Santos et al. (2020) developed. Results from both products indicated that the methodology produced similar patterns, showing peaks during dry seasons and lows in wet seasons, reflecting the pronounced precipitation characteristics of the Brazilian Cerrado (Figure 2.5). The irrigation depth and water uptake, as calculated using ET_{ALEXI} data (D_{ALEXI} and Q_{ALEXI}), were higher throughout the year than those derived from ET_{MODIS} (Figure 2.5). This discrepancy can be attributed to the higher ET values obtained from ET_{ALEXI}. As discussed earlier, ET_{MODIS} faces challenges in accurately estimating ET in the Cerrado region, leading to a tendency to underestimate values.

Moreover, the irrigation depth values obtained in this study align with those reported by farms in Western Bahia, as documented by Santos et al. (2020), indicating values of close to zero in the wet season and around 100 mm in the dry season using both ET products. However, unlike Santos et al. (2020), this study lacks data to compare the water conflict situation across all sub-basins in the RM irrigation zone. Indeed, the availability of environmental information, particularly water resources data, is much more limited in RM than in Western Bahia.

The findings of this study provide valuable support for future research on sustainable irrigation in Mato Grosso. The dataset presented here offers a preliminary insight into irrigation practices in the state, marking a fundamental step toward improved water resource management, particularly in small zones heavily occupied by irrigation. Additionally, applying a new ET dataset provided by the GLODET platform opens new possibilities for irrigation monitoring by remote sensing.

As announced by NASA, the Terra and Aqua satellites are reaching the end of their Earth Observation mission due to a depletion of fuel needed to maintain altitude and meet tight crossing times, 10:30 am for Terra and 1:30 pm for Aqua (Terra-Nasa, 2023). Both satellites are currently departing from their respective constellations, causing their local crossing times to drift earlier (Terra) and later (Aqua) in the day. Therefore, applying VIIRS data with a more consistent approach model, such as ALEXI, significantly improves capturing real field fluxes. As verified in this study, the new dataset demonstrates greater consistency in capturing fluxes that the MOD16 model underestimates.

However, an important limitation of this work is associated with validating ET remote sensing products. While I employed an eddy covariance tower for data validation situated in native vegetation, the reliability of the products in capturing energy fluxes requires additional towers in irrigation fields. All eddy covariance towers in Mato Grosso state are in natural vegetation land covers and none in irrigated fields. Additionally, despite using a higher

resolution product compared to the one used in Santos et al. (2020), the estimates of irrigation depth require ground truth data for validation. This database is still lacking in Mato Grosso.

2.5 Conclusion

The findings of this study represent an initial step toward understanding the irrigation situation in Mato Grosso. Furthermore, they emphasize the promising application of the ET dataset provided by a new remote sensing product obtained from the GLODET platform. This new ET dataset utilizes VIIRS data and integrates the ALEXI model, showing promise in enhancing the proposed monitoring system that relies on discontinued MODIS data. Moreover, VIIRS is the new standard operational radiometer for polar-orbit satellites, being launched onboard the NASA Suomi NPP (2011), the NOAA-20 (2017) and NOAA-21 (2022) satellites.

As revealed by the results, the new ET dataset demonstrates superior alignment with measurements from the flux tower when contrasted with previous MODIS data, which tends to underestimate ET values. However, further analyses are imperative, especially with an expanded network of towers in irrigated fields, to validate these observations.

Moreover, I emphasize the integration of irrigation discharge data produced here with river gauge data in the future. This analysis can provide significant insights into the water resources situation in RM, revealing areas with a higher probability of conflicts due to excessive irrigation. Additionally, this analysis can also assist in the identification of regions with potential for irrigation expansion by identifying basins with high water availability and low water demand.

General Conclusions

Irrigation is experiencing significant growth in Brazil. Beyond enhancing productivity, it plays a potential role in safeguarding crops by providing essential water supplementation during dry periods. However, the intensification of climate change introduces uncertainties in the duration and volume of rainfall, affecting the recharge of aquifers and rivers, crucial water resources for irrigation. This challenge becomes more pronounced in regions heavily occupied by irrigation, where competition for water resources can escalate into conflicts among users. To address these issues, monitoring the water demand for irrigation becomes essential. Such monitoring not only helps prevent conflicts but also guides both public and private entities in making decisions about when and where to implement irrigation. This thesis presented an in-depth analysis of the use of remote sensing technology to quantify the water demand for irrigation, particularly in Brazilian regions characterized by the widespread use of center pivot systems known as irrigation zones.

In the first chapter, a diagnosis of water resources was conducted in the basins of Corrente and Grande River located in the Western part of Bahia, an important irrigation zone in Brazil. In this study, the MOD16 product of the MODIS Global Evapotranspiration Project was used to calculate the water demand of center pivots mapped in the regions. The developed methodology integrated evapotranspiration, precipitation, and field data to estimate monthly irrigation demand across the entire basins for the period from 2001 to 2019. The results demonstrated the effectiveness of remote sensing in capturing irrigation patterns in the basins, revealing a growing use of water resources. Additionally, a comprehensive analysis of water demand data for irrigation, coupled with river gauge data, revealed that smaller sub-basins extensively occupied by center pivot experienced a higher frequency of conflicts throughout the time series.

Chapter two presents the water situation in another significant irrigation zone in Brazil, the Alto Rio das Mortes region, located in Mato Grosso. In this study, the use of a new evapotranspiration product obtained through remote sensing was investigated, the product provided by the GLODET platform (Global daily evapotranspiration), hosted by the Daugherty Water for Food Global Institute (DWFI) at the University of Nebraska. The introduction of this new product aimed to enhance the irrigation estimation method developed in the first chapter, providing new possibilities for assessing irrigation demand. The results indicated that, in comparison to MODIS data, the new product performed better in capturing evapotranspiration. As revealed, the MOD16 product tends to underestimate evapotranspiration values due to limitations in its model. Additionally, the study provided a historical series of monthly water demand for the region, covering the years from 2001 to 2022.

Therefore, this thesis provided crucial information that could address potential conflicts arising from the competition for water resources in regions heavily occupied by irrigation. Besides, it demonstrated the effectiveness of remote sensing technology, specifically the use of products like MOD16 and GLODET, in capturing and quantifying irrigation patterns. Considering the findings, I suggest the following points that should be prioritized for future enhancements:

- Explore methods for integrating additional remote sensing products with advanced data analytics to develop more precise monitoring systems.
- Incorporate ground truth data measured in irrigation fields, such as evapotranspiration and water use by center pivots. This could enhance the accuracy of irrigation demand estimation.
- Conduct a joint analysis of the estimated water demand for irrigation with river gauge data, especially focusing on the region analyzed in Chapter 2.

References

Aguilar, A. L., Flores, H., Crespo, G., Marín, M. I., Campos, I., & Calera, A. (2018). Performance assessment of MOD16 in evapotranspiration evaluation in Northwestern Mexico. Water (Switzerland), 10(7). https://doi.org/10.3390/w10070901

ANA, Agência Nacional de Águas. Atlas de Irrigação: Uso da Água na Agricultura. 2017. Available online: http://arquivos.ana.gov.br/imprensa/publicacoes/AtlasIrrigacao-UsodaAguanaAgriculturaIrrigada.pdf.

ANA, Agência Nacional de Águas e Saneamento Básico. Atlas Irrigação. Uso da água na agricultura irrigada. 2021. Available online: https://metadados.snirh.gov.br/geonetwork/srv/api/records/1b19cbb4-10fa-4be4-96db-b3dcd8975db0.

Allen, R. G., Pereira, L. S., Raes, D., & Smith, M. (1998). Crop evapotranspiration - Guidelines for computing crop water requirements -. Irrigation and Drainage Paper No. 56, FAO, 300. https://doi.org/10.1016/j.eja.2010.12.001

Allen, R. G., Tasumi, M., Morse, A., Trezza, R., Wright, J. L., Bastiaanssen, W., Kramber, W., Lorite, I., & Robison, C. W. (2007). Satellite-Based Energy Balance for Mapping Evapotranspiration with Internalized Calibration (METRIC)—Applications. Journal of Irrigation and Drainage Engineering, 133(4), 395–406. https://doi.org/10.1061/(asce)0733-9437(2007)133:4(395)

Anderson, M. C., Norman, J. M., Diak, G. R., Kustas, W. P., & Mecikalski, J. R. (1997). A two-source time-integrated model for estimating surface fluxes using thermal infrared remote sensing. Remote Sensing of Environment, 60(2), 195–216. https://doi.org/10.1016/S0034-4257(96)00215-5

Anderson, M. C., Norman, J. M., Mecikalski, J. R., Otkin, J. A., & Kustas, W. P. (2007a). A climatological study of evapotranspiration and moisture stress across the continental United States based on thermal remote sensing: 1. Model formulation. Journal of Geophysical Research Atmospheres, 112(10). https://doi.org/10.1029/2006JD007506

Anderson, M. C., Norman, J. M., Mecikalski, J. R., Otkin, J. A., & Kustas, W. P. (2007b). A climatological study of evapotranspiration and moisture stress across the continental United

States based on thermal remote sensing: 2. Surface moisture climatology. Journal of Geophysical Research Atmospheres, 112(11). https://doi.org/10.1029/2006JD007507

Barbosa, H. A., Huete, A. R., & Baethgen, W. E. (2006). A 20-year study of NDVI variability over the Northeast Region of Brazil. Journal of Arid Environments, 67(2), 288–307. https://doi.org/10.1016/j.jaridenv.2006.02.022

Bastiaanssen W.G.M., M. Meneti, R.A. Feddes, & Holtslag, a a M. (1998). A remote sensing surface energy balance algorithm for land (SEBAL). Journal of Hydrology, 212–213, 198–212.

Bazzi, H., Baghdadi, N., Ienco, D., Hajj, M. El, Zribi, M., Belhouchette, H., Escorihuela, M. J., & Demarez, V. (2019). Mapping irrigated areas using Sentinel-1 time series in Catalonia, Spain. Remote Sensing, 11(15), 1–25. https://doi.org/10.3390/rs11151836

Bernardo, S.; Mantovani, E.C.; Da Silva, D.D.; Soares, A.A. Manual de Irrigação, 9th ed.; Editora UFV:Viçosa, Brazil, 2019; ISBN 9788572696104

Biggs, T. W., Marshall, M., & Messina, A. (2016). Mapping daily and seasonal evapotranspiration from irrigated crops using global climate grids and satellite imagery: Automation and methods comparison. Water Resources Research, 52(9), 7311–7326. https://doi.org/10.1002/2016WR019107

Bispo, R. C., Hernandez, F. B. T., Gonçalves, I. Z., Neale, C. M. U., & Teixeira, A. H. C. (2022). Remote sensing based evapotranspiration modeling for sugarcane in Brazil using a hybrid approach. Agricultural Water Management, 271. https://doi.org/10.1016/j.agwat.2022.107763

Biudes, M. S., Geli, H. M. E., Vourlitis, G. L., Machado, N. G., Pavão, V. M., Dos Santos, L. O. F., & Querino, C. A. S. (2022). Evapotranspiration Seasonality over Tropical Ecosystems in Mato Grosso, Brazil. Remote Sensing, 14(10). https://doi.org/10.3390/rs14102482

Brocca, L., Tarpanelli, A., Filippucci, P., Dorigo, W., Zaussinger, F., Gruber, A., & Fernández-Prieto, D. (2018). How much water is used for irrigation? A new approach exploiting coarse resolution satellite soil moisture products. International Journal of Applied Earth Observation and Geoinformation, 73(August), 752–766. https://doi.org/10.1016/j.jag.2018.08.023

Brust, C., Kimball, J. S., Maneta, M. P., Jencso, K., He, M., & Reichle, R. H. (2021). Using SMAP Level-4 soil moisture to constrain MOD16 evapotranspiration over the contiguous USA. Remote Sensing of Environment, 255. https://doi.org/10.1016/j.rse.2020.112277

Cambraia Neto, A. J., Rodrigues, L. N., da Silva, D. D., & Althoff, D. (2021). Impact of climate change on groundwater recharge in a Brazilian Savannah watershed. Theoretical and Applied Climatology, 143(3–4), 1425–1436. https://doi.org/10.1007/s00704-020-03477-w

Cheng, L., Yang, M., Wang, X., & Wan, G. (2020). Spatial and Temporal Variations of Terrestrial Evapotranspiration in the Upper Taohe River Basin from 2001 to 2018 Based on MOD16 ET Data. Advances in Meteorology, 2020, 1–17. https://doi.org/10.1155/2020/3721414

CBHRC. Deliberação. 2015. Available online: https://www.conjur.com.br/dl/deliberacao-comite-bacia-corrente.pdf

Coelho, E. F., Coelho Filho, M. A. C., & Oliveira, S. L. De. (2005). Agricultura irrigada : eficiência de irrigação e de uso de água. Bahia Agrícola, 7, 57–60.

CONAB. Companhia Nacional de Abastecimento. Série histórica de produção de grãos. 2023. Available online: https://www.conab.gov.br/info-agro/safras/serie-historica-das-safras#gr%C3%A3os-2.

Costa, M. H., Fleck, L. C., Cohn, A. S., Abrahão, G. M., Brando, P. M., Coe, M. T., Fu, R., Lawrence, D., Pires, G. F., Pousa, R., & Soares-Filho, B. S. (2019). Climate risks to Amazon agriculture suggest a rationale to conserve local ecosystems. Frontiers in Ecology and the Environment, 17(10), 584–590. https://doi.org/10.1002/fee.2124

Funk, C., Peterson, P., Landsfeld, M., Pedreros, D., Verdin, J., Shukla, S., Husak, G., Rowland, J., Harrison, L., Hoell, A., & Michaelsen, J. (2015). The climate hazards infrared precipitation with stations - A new environmental record for monitoring extremes. Scientific Data, 2. https://doi.org/10.1038/sdata.2015.66

GLODET, Global Daily Evapo-Transpiration, 2023. Available online: https://glodet.nebraska.edu/#/

GESDISC. Goddard Earth Sciences Data and Information Services Center. 2020. Available online: https://disc.gsfc.nasa.gov/datasets/TRMM_3B42_Daily_7/summary

Gonçalves, I. Z., Ruhoff, A., Laipelt, L., Bispo, R., Hernandez, F. B. T., Neale, C. M. U., Teixeira, A. H. de C., & Marin, F. R. (2022). Remote Sensing-Based Evapotranspiration Modeling Using Geesebal for Sugarcane Irrigation Management in Brazil. SSRN Electronic Journal. https://doi.org/10.2139/ssrn.4162286

Hain, C. R., & Anderson, M. C. (2017). Estimating morning change in land surface temperature from MODIS day/night observations: Applications for surface energy balance modeling. Geophysical Research Letters, 44(19), 9723–9733. https://doi.org/10.1002/2017GL074952

Hofmann, G. S., Silva, R. C., Weber, E. J., Barbosa, A. A., Oliveira, L. F. B., Alves, R. J. V., Hasenack, H., Schossler, V., Aquino, F. E., & Cardoso, M. F. (2023). Changes in atmospheric circulation and evapotranspiration are reducing rainfall in the Brazilian Cerrado. Scientific Reports, 13(1). https://doi.org/10.1038/s41598-023-38174-x

Jalilvand, E., Tajrishy, M., Ghazi Zadeh Hashemi, S. A., & Brocca, L. (2019). Quantification of irrigation water using remote sensing of soil moisture in a semi-arid region. Remote Sensing of Environment, 231(May), 111226. https://doi.org/10.1016/j.rse.2019.111226

Karthikeyan, L., Chawla, I., & Mishra, A. K. (2020). A review of remote sensing applications in agriculture for food security: Crop growth and yield, irrigation, and crop losses. Journal of Hydrology, 586(March), 124905. https://doi.org/10.1016/j.jhydrol.2020.124905

Kustas, W. P. (1990). Estimates of Evapotranspiration with One- and Two- Layer Model of Heat Tranfer over Partial Canopy Cover. Journal of Applied Meteorology, 29, 704–715.

Leite-Filho, A. T., Soares-Filho, B. S., Davis, J. L., Abrahão, G. M., & Börner, J. (2021). Deforestation reduces rainfall and agricultural revenues in the Brazilian Amazon. Nature Communications, 12(1). https://doi.org/10.1038/s41467-021-22840-7

Luiz Silva, W., Xavier, L. N. R., Maceira, M. E. P., & Rotunno, O. C. (2019). Climatological and hydrological patterns and verified trends in precipitation and streamflow in the basins of Brazilian hydroelectric plants. Theoretical and Applied Climatology, 137(1–2), 353–371. https://doi.org/10.1007/s00704-018-2600-8

Mantovani, E.C.; Bernardo, S.; Palaretti, L.F. Irrigação: Princípios e Métodos, 3rd ed.; Editora UFV: Viçosa, Brazil, 2009; ISBN 9788572693738.

MAPBIOMAS. 2023. Available online: https://brasil.mapbiomas.org/

Marques, E. A. G., Silva Junior, G. C., Eger, G. Z. S., Ilambwetsi, A. M., Raphael, P., Generoso, T. N., Oliveira, J., & Júnior, J. N. (2020). Analysis of groundwater and river stage fluctuations and their relationship with water use and climate variation effects on Alto Grande watershed, Northeastern Brazil. Journal of South American Earth Sciences, 103, 102723. https://doi.org/10.1016/j.jsames.2020.102723

Michel, D., Jiménez, C., Miralles, D. G., Jung, M., Hirschi, M., Ershadi, A., Martens, B., Mccabe, M. F., Fisher, J. B., Mu, Q., Seneviratne, S. I., Wood, E. F., & Fernández-Prieto, D. (2016). The WACMOS-ET project - Part 1: Tower-scale evaluation of four remote-sensing-based evapotranspiration algorithms. Hydrology and Earth System Sciences, 20(2), 803–822. https://doi.org/10.5194/hess-20-803-2016

Miralles, D. G., Jiménez, C., Jung, M., Michel, D., Ershadi, A., Mccabe, M. F., Hirschi, M., Martens, B., Dolman, A. J., Fisher, J. B., Mu, Q., Seneviratne, S. I., Wood, E. F., & Fernández-Prieto, D. (2016). The WACMOS-ET project - Part 2: Evaluation of global terrestrial evaporation data sets. Hydrology and Earth System Sciences, 20(2), 823–842. https://doi.org/10.5194/hess-20-823-2016

Mu, Q., Heinsch, F. A., Zhao, M., & Running, S. W. (2007). Development of a global evapotranspiration algorithm based on MODIS and global meteorology data. Remote Sensing of Environment, 111(4), 519–536. https://doi.org/10.1016/j.rse.2007.04.015

Mu, Q., Zhao, M., & Running, S. W. (2011). Improvements to a MODIS global terrestrial evapotranspiration algorithm. Remote Sensing of Environment, 115(8), 1781–1800. https://doi.org/10.1016/j.rse.2011.02.019

Mu, Q., Zhao, M., & Running, S. W. (2013). MODIS Global Terrestrial Evapotranspiration (ET) Product (MOD16A2/A3). Algorithm Theoretical Basis Document, Collection, 66.

NASA. MODIS – Moderate Resolution Imaging Spectroradiometer. 2023. Available online: https://modis.gsfc.nasa.gov/

Neale, C. M. U., Geli, H. M. E., Kustas, W. P., Alfieri, J. G., Gowda, P. H., Evett, S. R., Prueger, J. H., Hipps, L. E., Dulaney, W. P., Chávez, J. L., French, A. N., & Howell, T. A. (2012). Soil water content estimation using a remote sensing-based hybrid evapotranspiration modeling approach. Advances in Water Resources, 50, 152–161. https://doi.org/10.1016/j.advwatres.2012.10.008

Norman, J. M., Kustas, W. P., & Humes, K. S. (1995). Source approach for estimating soil and vegetation energy fluxes in observations of directional radiometric surface temperature. Agricultural and Forest Meteorology, 77(3–4), 263–293. https://doi.org/10.1016/0168-1923(95)02265-Y

Peel, M.C., Finlayson, B. L., Mcmahon, T. A. (2007). Updated world map of the Köppen-Geiger climate classification. Hydrol. Earth Syst. Sci., 1633-1644. https://doi.org/10.5194/hess-11-1633-2007

Peña-Arancibia, J. L., Mainuddin, M., Kirby, J. M., Chiew, F. H. S., McVicar, T. R., & Vaze, J. (2016). Assessing irrigated agriculture's surface water and groundwater consumption by combining satellite remote sensing and hydrologic modelling. Science of the Total Environment, 542, 372–382. https://doi.org/10.1016/j.scitotenv.2015.10.086

Peña-Arancibia, J. L., McVicar, T. R., Paydar, Z., Li, L., Guerschman, J. P., Donohue, R. J., Dutta, D., Podger, G. M., van Dijk, A. I. J. M., & Chiew, F. H. S. (2014). Dynamic identification of summer cropping irrigated areas in a large basin experiencing extreme climatic variability. Remote Sensing of Environment, 154, 139–152. https://doi.org/10.1016/j.rse.2014.08.016

Pereira, O., Ferreira, L., Pinto, F., & Baumgarten, L. (2018). Assessing Pasture Degradation in the Brazilian Cerrado Based on the Analysis of MODIS NDVI Time-Series. Remote Sensing, 10(11), 1761. https://doi.org/10.3390/rs10111761

Pereira, B. H. F., Dereczynski, C., da Silva Junior, G. C., & Marques, E. A. G. (2022). Projected climate change impacts on groundwater recharge in the Urucuia aquifer system, Brazil. International Journal of Climatology, 42(16), 8822–8838. https://doi.org/10.1002/joc.7773

Pousa, R., Costa, M. H., Pimenta, F. M., Fontes, V. C., & Castro, M. (2019). Climate change and intense irrigation growth in Western Bahia, Brazil: The urgent need for hydroclimatic monitoring. Water (Switzerland), 11(5). https://doi.org/10.3390/w11050933

Pun, M., Mutiibwa, D., & Li, R. (2017). Land use classification: A surface energy balance and vegetation index application to map and monitor irrigated lands. Remote Sensing, 9(12). https://doi.org/10.3390/rs9121256

Radar Agro. 2023. Available online: https://blog.itau.com.br/ibba

Ramoelo, A., Majozi, N., Mathieu, R., Jovanovic, N., Nickless, A., & Dzikiti, S. (2014). Validation of global evapotranspiration product (MOD16) using flux tower data in the African savanna, South Africa. Remote Sensing, 6(8), 7406–7423. https://doi.org/10.3390/rs6087406

Rocha Junior, A. B., Barretto, A. G. de O. P., Chamma, A. L. S., Fendrich, A. N., Gianetti, G. W., Safanelli, J. L., et al. 2020. Análise Territorial para o Desenvolvimento da Agricultura

Irrigada no Brasil: Plano de Ação Imediata da Agricultura Irrigada no Brasil para o período 2020-2023. Piracicaba, SP: Grupo de Políticas Públicas. ESALQ/USP.

Rodrigues, J. A. M., Viola, M. R., Alvarenga, L. A., de Mello, C. R., Chou, S. C., Oliveira, V. A., Uddameri, V., & Morais, M. A. V. (2019). Climate change impacts under RCP scenarios on streamflow and droughts of basins in the Brazilian Cerrado Biome. International Journal of Climatology, 40(5), 2511–2526. https://doi.org/https://doi.org/10.1002/joc.6347

Roerink, G. J., Su, Z., & Menenti, M. (2000). S-SEBI: A simple remote sensing algorithm to estimate the surface energy balance. Physics and Chemistry of the Earth, Part B: Hydrology, Oceans and Atmosphere, 25(2), 147–157. https://doi.org/10.1016/S1464-1909(99)00128-8

Rosa, L. (2022). Adapting agriculture to climate change via sustainable irrigation: Biophysical potentials and feedbacks. In Environmental Research Letters (Vol. 17, Issue 6). Institute of Physics. https://doi.org/10.1088/1748-9326/ac7408

Salazar-Martínez, D., Holwerda, F., Holmes, T. R. H., Yépez, E. A., Hain, C. R., Alvarado-Barrientos, S., Ángeles-Pérez, G., Arredondo-Moreno, T., Delgado-Balbuena, J., Figueroa-Espinoza, B., Garatuza-Payán, J., González del Castillo, E., Rodríguez, J. C., Rojas-Robles, N. E., Uuh-Sonda, J. M., & Vivoni, E. R. (2022). Evaluation of remote sensing-based evapotranspiration products at low-latitude eddy covariance sites. Journal of Hydrology, 610. https://doi.org/10.1016/j.jhydrol.2022.127786

Salmona, Y. B., Matricardi, E. A. T., Skole, D. L., Silva, J. F. A., Coelho Filho, O. de A., Pedlowski, M. A., Sampaio, J. M., Castrillón, L. C. R., Brandão, R. A., Silva, A. L. da, & Souza, S. A. de. (2023). A Worrying Future for River Flows in the Brazilian Cerrado Provoked by Land Use and Climate Changes. Sustainability (Switzerland), 15(5). https://doi.org/10.3390/su15054251

Santos, A. B., Costa, M. H., Mantovani, E. C., Boninsenha, I., & Castro, M. (2020). A remote sensing diagnosis of water use and water stress in a region with intense irrigation growth in brazil. Remote Sensing, 12(22), 1–16. https://doi.org/10.3390/rs12223725

Saraiva, M., Protas, É., Salgado, M., & Souza, C. (2020). Automatic mapping of center pivot irrigation systems from satellite images using deep learning. Remote Sensing, 12(3), 1–14. https://doi.org/10.3390/rs12030558

Souza, V. de A., Roberti, D. R., Ruhoff, A. L., Zimmer, T., Adamatti, D. S., de Gonçalves, L. G. G., Diaz, M. B., Alves, R. de C. M., & de Moraes, O. L. L. (2019). Evaluation of MOD16

algorithm over irrigated rice paddy using flux tower measurements in Southern Brazil. Water (Switzerland), 11(9). https://doi.org/10.3390/w11091911

Su, Z. (2002). The Surface Energy Balance System (SEBS) for estimation of turbulent heat fluxes. Hydrology and Earth System Sciences, 6(1), 85–99.

Terra-NASA. Maintaining Terra and Aqua MODIS Continuity. 2023. Available online: https://modis.gsfc.nasa.gov/sci_team/meetings/202211/presentations.php

Twine, T. E., Kustas, W. P., Norman, J. M., Cook, D. R., Houser, P. R., Meyers, T. P., Prueger, J. H., Starks, P. J., & Wesely, M. L. (2000). Correcting eddy-covariance flux underestimates over a grassland. Agricultural and Forest Meteorology, 103, 279–300.

Wutzler, T., Lucas-Moffat, A., Migliavacca, M., Knauer, J., Sickel, K., Šigut, L., Menzer, O., & Reichstein, M. (2018). Basic and extensible post-processing of eddy covariance flux data with REddyProc. Biogeosciences, 15(16), 5015–5030. https://doi.org/10.5194/bg-15-5015-2018

Zhang, K., Kimball, J. S., & Running, S. W. (2016). A review of remote sensing based actual evapotranspiration estimation. Wiley Interdisciplinary Reviews: Water, 3(6), 834–853. https://doi.org/10.1002/wat2.1168